Electronic Supplementary Information

Retro Baeyer–Villiger reaction: thermal conversion of the [60]fullerene-fused lactones to ketones

Chuang Niu,‡[a] Zheng-Chun Yin,‡[a] Wei-Feng Wang,[a] Xinmin Huang,[a] Dian-Bing Zhou,[a] Guan-Wu Wang[a,b,*]

[a] *Hefei National Laboratory for Physical Sciences at Microscale and Department of Chemistry, University of Science and Technology of China, Hefei, Anhui 230026, P. R. China E-mail: gwang@ustc.edu.cn; Fax: +86 551 3607864; Tel: +86 551 3607864*
[b] *State Key Laboratory of Applied Organic Chemistry, Lanzhou University, Lanzhou, Gansu 730000, P. R. China*
‡ *These authors contributed equally to this work.*

Table of Contents

1. General Information

Compounds **1a**–**i** were synthesized according to the procedure developed by our group.[1] Tetra-*n*-butylammonium perchlorate (TBAP) was recrystallized from absolute ethanol and dried in a vacuum at 313 K prior to use. Other chemicals were obtained commercially and used without further purification. ^{1}H NMR and ^{13}C NMR spectra were recorded on a Bruker ASCEND III–400 or a Bruker ASCEND III–500 spectrometer at room temperature. ^{1}H NMR and ^{13}C NMR chemical shifts were determined relative to TMS. Abbreviations for signal couplings are: s, singlet; d, doublet; t, triplet; m, multiplet. Compounds **2a**–**f**, **2h** and **2i** are known compounds, and their ^{1}H NMR data are consistent with those reported in the literature.[2] High resolution mass spectra were obtained on a Bruker UltrafleXtreme MALDI-TOF/TOF instrument. UV-vis spectra were obtained on a SHIMADZU UV-3600PLUS instrument. IR spectra were obtained on a Thermo Scientific Nicolet 6700 instrument. All electrochemical reactions, CV and DPV measurements were performed under an argon atmosphere using a Shanghai Chenhua CHI630D workstation.

2. Synthesis and Spectral Data of Compounds 2a–i

General Procedure: A dry 25 mL tube equipped with a magnetic stirrer was charged with **1** (0.015 mmol) and triflic anhydride (Tf_2O) (0.045–0.150 mmol), which were dissolved in anhydrous 1,2-dichlorobenzene (1,2-$C_6H_4Cl_2$) (3 mL) under an air atmosphere. Then, the tube was sealed tightly and stirred in an oil bath at 120 °C for 10 h. The resulting mixture was filtered through a silica gel (200–300 mesh) plug with CS_2/CH_2Cl_2 (1:1 v/v) to remove insoluble materials. After the solvent had been evaporated in *vacuo*, the residue was separated on a silica gel column (300–400 mesh) with CS_2/CH_2Cl_2 (4:1 v/v) as the eluent to give product **2**.

2.1. Synthesis of 2a

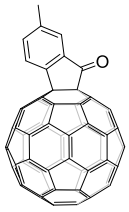

2a

By following the general procedure, the reaction of **1a** (12.8 mg, 0.015 mmol) and Tf_2O (7.5 μL, 0.045 mmol) in 1,2-$C_6H_4Cl_2$ (3 mL) at 120 °C for 10 h afforded **2a** (10.9 mg, 87%): amorphous brown solid; ^{1}H NMR (400 MHz, 1:1 $CS_2/CDCl_3$) δ 8.37 (d, J = 7.9 Hz, 1H), 8.21 (s, 1H), 7.87 (dd, J = 7.9, 1.1 Hz, 1H), 2.72 (s, 3H).

2.2. Synthesis of 2b

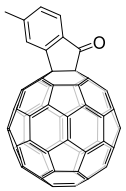

2b

By following the general procedure, the reaction of **1b** (12.8 mg, 0.015 mmol) and Tf_2O (7.5 μL, 0.045 mmol) in 1,2-$C_6H_4Cl_2$ (3 mL) at 120 °C for 10 h afforded **2b** (11.2 mg, 89%): amorphous brown solid; ^{1}H NMR (400 MHz, 1:1 CS_2/$CDCl_3$) δ 8.32 (d, J = 8.1 Hz, 1H), 8.30 (s, 1H), 7.66 (dd, J = 7.9, 0.6 Hz, 1H), 2.72 (s, 3H).

2.3. Synthesis of 2c

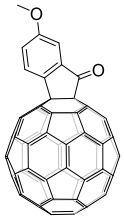

2c

By following the general procedure, the reaction of **1c** (13.1 mg, 0.015 mmol) and Tf_2O (12.5 μL, 0.075 mmol) in 1,2-$C_6H_4Cl_2$ (3 mL) at 120 °C for 10 h afforded **2c** (11.3 mg, 88%): amorphous brown solid; ^{1}H NMR (400 MHz, 1:1 CS_2/$CDCl_3$) δ 8.34 (d, J = 8.5 Hz, 1H), 7.79 (d, J = 2.6 Hz, 1H), 7.61 (dd, J = 8.5, 2.6 Hz, 1H), 4.09 (s, 3H).

2.4. Synthesis of 2d

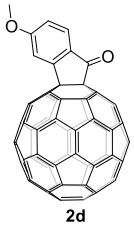

2d

By following the general procedure, the reaction of **1d** (13.1 mg, 0.015 mmol) and Tf_2O (12.5 μL, 0.075 mmol) in 1,2-$C_6H_4Cl_2$ (3 mL) at 120 °C for 10 h afforded **2d** (11.1 mg, 86%): amorphous brown solid; ^{1}H NMR (400 MHz, 1:1 CS_2/$CDCl_3$) δ 8.31 (d, J = 8.6 Hz, 1H), 7.86 (d, J = 2.2 Hz, 1H), 7.35 (dd, J = 8.6, 2.2 Hz, 1H), 4.08 (s, 3H).

2.5. Synthesis of 2e

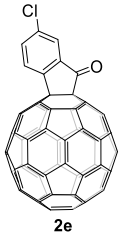

2e

By following the general procedure, the reaction of **1e** (13.1 mg, 0.015 mmol) and Tf_2O (25.0 μL, 0.150 mmol) in 1,2-$C_6H_4Cl_2$ (3 mL) at 120 °C for 10 h afforded **2e** (10.5 mg, 81%): amorphous brown solid; ^{1}H NMR (400 MHz, 1:1 CS_2/$CDCl_3$) δ 8.43 (d, J = 8.2 Hz, 1H), 8.36 (d, J = 2.0 Hz, 1H), 7.99 (dd, J = 8.2, 2.0 Hz, 1H).

2.6. Synthesis of 2f

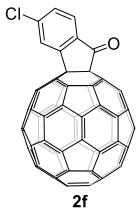

2f

By following the general procedure, the reaction of **1f** (13.1 mg, 0.015 mmol) and Tf_2O (25.0 μL, 0.150 mmol) in 1,2-$C_6H_4Cl_2$ (3 mL) at 120 ºC for 10 h afforded **2f** (10.6 mg, 82%): amorphous brown solid; ^{1}H NMR (400 MHz, 1:1 CS_2/$CDCl_3$) δ 8.47 (d, J = 1.7 Hz, 1H), 8.34 (d, J = 8.2 Hz, 1H), 7.81 (dd, J = 8.2, 1.7 Hz, 1H).

2.7. Synthesis of 2g

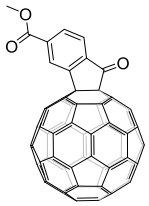

2g

By following the general procedure, the reaction of **1g** (13.4 mg, 0.015 mmol) and Tf_2O (12.5 μL, 0.075 mmol) in 1,2-$C_6H_4Cl_2$ (3 mL) at 120 ºC for 10 h afforded **2g** (10.5 mg, 80%): amorphous brown solid; ^{1}H NMR (500 MHz, 1:1 CS_2/$CDCl_3$) δ 9.11 (s, 1H), 8.50 (d, J = 7.9 Hz, 1H), 8.49 (d, J = 7.9 Hz, 1H), 4.04 (s, 3H); ^{13}C NMR (126 MHz, 1:1 CS_2/$CDCl_3$) (all 2C unless indicated) δ 198.30 (*C*=*O*), 165.15 (*C*=*O*), 156.36, 153.39, 152.78, 147.38 (1C), 147.35, 147.14 (1C), 146.36 (4C), 146.10, 146.06, 145.71, 145.61, 145.54, 145.47, 145.37, 145.34, 144.55, 144.23, 143.08, 142.73, 142.67, 142.35, 142.08, 142.03, 142.00, 141.91, 141.57, 140.59, 140.56, 137.91 (1C, aryl *C*), 137.52 (1C, aryl *C*), 135.51 (1C, aryl *C*), 135.43, 131.11 (1C, aryl *C*), 128.00 (1C, aryl *C*), 127.17 (1C, aryl *C*), 78.74 (1C, sp^3-*C* of C_{60}), 70.62 (1C, sp^3-*C* of C_{60}), 52.75 (1C); FT-IR ν/cm^{-1} (KBr) 1727, 1608, 1588, 1513, 1433, 1414, 1285, 1214, 1137, 1100, 1079, 1013, 987, 850, 833, 800, 765, 728, 687, 553, 527; UV-vis ($CHCl_3$) λ_{max}/nm (log ε) 258 (5.06), 310 (4.55), 430 (3.54), 697 (2.52); MALDI-TOF MS *m/z* calcd for $C_{69}H_6O_3$ [M]$^-$ 882.0322, found 882.0316.

2.8. Synthesis of 2h

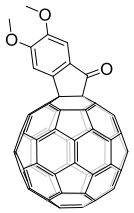

2h

By following the general procedure, the reaction of **1h** (13.5 mg, 0.015 mmol) and Tf_2O (12.5 μL, 0.075 mmol) in 1,2-$C_6H_4Cl_2$ (3 mL) at 120 ºC for 3 h afforded **2h** (10.9 mg, 82%): amorphous brown solid; ^{1}H NMR (400 MHz, 1:1 CS_2/$CDCl_3$) δ 7.80 (s, 1H), 7.75 (s, 1H), 4.15 (s, 3H), 4.14 (s, 3H).

2.9. Synthesis of 2i

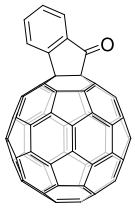

2i

By following the general procedure, the reaction of **1i** (12.6 mg, 0.015 mmol) and Tf_2O (7.5 μL, 0.045 mmol) in 1,2-$C_6H_4Cl_2$ (3 mL) at 120 °C for 10 h afforded **2i** (11.1 mg, 90%): amorphous brown solid; ^{1}H NMR (400 MHz, 1:1 CS_2/$CDCl_3$) δ 8.50 (d, J = 7.8 Hz, 1H), 8.42 (d, J = 7.7 Hz, 1H), 8.06 (td, J = 7.5, 1.2 Hz, 1H), 7.85 (td, J = 7.5, 0.8 Hz, 1H).

3. Synthesis and Spectral Data of Compounds 3a–5a

3.1. Synthesis of 3a and 4a

Compound **2a** (12.6 mg, 0.015 mmol) was electroreduced by controlled potential electrolysis (CPE) at –1.30 V vs. saturated calomel electrode (SCE) in 15 mL of 1,2-$C_6H_4Cl_2$ containing 0.1 M TBAP under an argon atmosphere at room temperature. The electrolysis was terminated when the theoretical number of coulombs required for a full conversion of **2a** to **2a**$^{2-}$ was reached. Then, the dianionic **2a**$^{2-}$ was allowed to react with benzyl bromide ($PhCH_2Br$) (134.1 μL, 1.125 mmol) and sodium hydride (NaH) (57–63% oil dispersion, 31.2 mg, 0.75 mmol). After being stirred at 50 °C for 6 h, the resulting mixture was directly filtered through a silica gel (200–300 mesh) plug with CS_2/CH_2Cl_2 (1:1 v/v) to remove the supporting electrolyte and insoluble materials, and then evaporated in *vacuo* to remove the solvent. Next, the residue was further separated on a silica gel column (300–400 mesh) with CS_2 as the eluent to afford product **3a** (5.0 mg, 29%) and product **4a** (4.4 mg, 25%) as amorphous brown solids.

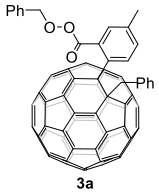

3a

Compound 3a: ^{1}H NMR (500 MHz, 1:1 CS_2/$CDCl_3$) δ 8.60 (d, J = 8.0 Hz, 1H), 7.62 (d, J = 8.0 Hz, 1H), 7.58 (s, 1H), 7.40–7.24 (m, 7H), 7.15–7.06 (m, 3H), 5.47 (d, J = 12.3 Hz, 1H), 5.43 (d, J = 12.3 Hz, 1H), 4.93 (d, J = 12.3 Hz, 1H), 4.04 (d, J = 12.3 Hz, 1H), 2.55 (s, 3H); ^{13}C NMR (126 MHz, 1:1 CS_2/$CDCl_3$) (all 1C unless indicated) δ 170.07 (*C*=*O*), 157.04, 156.68, 154.94, 153.16, 147.85, 147.64, 147.20, 146.73, 146.58 (2C), 146.56, 146.52, 146.39, 146.32, 146.25, 146.19, 146.03, 146.00, 145.88, 145.63, 145.62, 145.55 (2C), 145.47, 145.36, 145.31, 145.28, 145.03, 144.77 (2C), 144.58, 144.26, 143.38, 143.26, 142.74, 142.69, 142.67 (2C), 142.41, 142.30, 142.28 (2C), 142.08, 142.04, 141.57, 141.53, 141.44, 141.39, 141.23, 140.46, 139.77, 139.57, 138.96, 138.72, 138.50, 138.38 (aryl *C*), 137.84 (aryl *C*), 137.01 (aryl *C*), 136.67,

135.23 (aryl *C*), 135.06 (aryl *C*), 134.68, 134.11 (aryl *C*), 133.84, 132.05 (2C, aryl *C*), 131.36 (aryl *C*), 130.43 (aryl *C*), 128.87 (2C, aryl *C*), 128.69 (2C, aryl *C*), 128.61 (aryl *C*), 127.92 (2C, aryl *C*), 126.88 (aryl *C*), 71.52 (sp^3-*C* of C_{60}), 67.98, 67.36 (sp^3-*C* of C_{60}), 49.12, 21.18; FT-IR ν/cm^{-1} (KBr) 1718, 1492, 1450, 1290, 1251, 1203, 1147, 1090, 1063, 817, 748, 733, 695, 576, 525; UV-vis ($CHCl_3$) λ_{max}/nm (log ε) 258 (5.08), 314 (4.67), 436 (3.61), 705 (2.70); MALDI-TOF MS *m/z* calcd for $C_{82}H_{20}O_3$ $[M]^-$ 1152.1418, found 1152.1416.

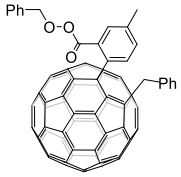

4a

Compound 4a: ^{1}H NMR (500 MHz, 1:1 CS_2/$CDCl_3$) δ 8.50 (d, J = 8.1 Hz, 1H), 7.52 (dd, J = 8.1, 1.3 Hz, 1H), 7.42 (d, J = 7.1 Hz, 2H), 7.37–7.27 (m, 7H), 7.23–7.16 (m, 2H), 5.26 (d, J = 12.4 Hz, 1H), 5.18 (d, J = 12.4 Hz, 1H), 4.17 (d, J = 13.0 Hz, 1H), 4.02 (d, J = 13.0 Hz, 1H), 2.53 (s, 3H); ^{13}C NMR (126 MHz, 1:1 CS_2/$CDCl_3$) (all 1C unless indicated) δ 169.38 (*C*=*O*), 156.21, 155.93, 151.09, 149.91, 148.89, 148.60, 148.43, 148.02, 147.36, 147.02 (2C), 147.01, 146.95, 146.90, 146.81 (2C), 146.76, 146.73, 145.45, 145.39, 145.18, 145.07, 144.99, 144.85, 144.56, 144.40, 144.37, 144.29, 144.23 (3C), 144.20, 144.01 (2C), 143.82, 143.71, 143.64, 143.61, 143.39, 143.20, 143.13, 143.06, 143.01, 142.92, 142.76, 142.66, 142.63, 142.52, 142.37 (2C), 142.17, 141.97, 141.89, 141.57, 140.69, 139.19, 138.57, 138.30, 137.98 (aryl *C*), 137.73, 135.37 (aryl *C*), 135.05 (aryl *C*), 134.08 (aryl *C*), 133.39 (aryl *C*), 131.30 (aryl *C*), 130.55 (2C, aryl *C*), 129.63 (aryl *C*), 129.49 (aryl *C*), 128.58 (2C, aryl *C*), 128.32 (aryl *C*), 128.30 (2C, aryl *C*), 128.18 (2C, aryl *C*), 127.08 (aryl *C*), 67.45, 60.24 (sp^3-*C* of C_{60}), 60.07 (sp^3-*C* of C_{60}), 47.76, 20.99; FT-IR ν/cm^{-1} (KBr) 1717, 1491, 1453, 1292, 1253, 1206, 1143, 1063, 819, 747, 729, 697, 578, 524; UV-vis ($CHCl_3$) λ_{max}/nm (log ε) 258 (5.05), 330 (4.54), 445 (3.81), 690 (2.48); MALDI-TOF MS *m/z* calcd for $C_{82}H_{20}O_3$ $[M]^-$ 1152.1418, found 1152.1412.

3.2. Synthesis of 5a

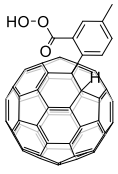

5a

Compound **2a** (16.8 mg, 0.020 mmol) was electroreduced by CPE at –1.30 V vs. SCE in 15 mL of 1,2-$C_6H_4Cl_2$ containing 0.1 M TBAP under an argon atmosphere at room temperature. The electrolysis was terminated when the theoretical number of coulombs required for a full conversion of **2a** to $\mathbf{2a}^{2-}$ was reached. Then, the dianionic $\mathbf{2a}^{2-}$ was allowed to react with trifluoroacetic acid (TFA) (4.5 μL, 0.060 mmol). After being stirred at 25 °C for 0.5 h, the resulting mixture was directly filtered through a neutral silica gel (200–300 mesh, pH: 6.5~7.5) plug with CS_2/ethyl acetate (5:1 v/v) to

remove the supporting electrolyte and insoluble materials, and then evaporated in *vacuo* to remove the solvent. Next, the residue was further separated on a neutral silica gel column (200–300 mesh, pH: 6.5~7.5) with CS_2/ethyl acetate (5:1 v/v) as the eluent to afford product **5a** (9.3 mg, 53%) as amorphous brown solid; ^{1}H NMR (400 MHz, 1:1 $CS_2/CDCl_3$) δ 8.51 (d, J = 8.0 Hz, 1H), 7.85 (s, 1H), 7.64 (dd, J = 8.0, 1.1 Hz, 1H), 6.90 (s, 1H), 2.57 (s, 3H); ^{13}C NMR (126 MHz, 1:1 $CS_2/CDCl_3$) (all 2C unless indicated) δ 174.30 (1C, *C*=*O*), 153.00 (4C), 147.44 (1C), 147.06 (1C), 146.85, 146.28, 146.21, 146.02 (6C), 145.67, 145.48, 145.31, 145.26, 145.20, 144.70, 144.34, 143.20, 142.46 (4C), 141.97, 141.95, 141.92, 141.83, 141.54, 141.41, 140.91, 140.07, 139.69, 138.10, 136.70 (1C, aryl *C*), 132.83 (1C, aryl *C*), 131.93 (1C, aryl *C*), 131.68 (1C, aryl *C*), 131.43 (1C, aryl *C*), 127.53 (1C, aryl *C*), 67.26 (1C, sp^3-*C* of C_{60}), 61.83 (1C, sp^3-*C* of C_{60}), 20.96 (1C); FT-IR ν/cm^{-1} (KBr) 1698, 1512, 1461, 1425, 1258, 1215, 1038, 886, 834, 819, 769, 642, 585, 525; UV-vis ($CHCl_3$) λ_{max}/nm (log ε) 255 (4.98), 330 (4.49), 430 (3.58), 704 (2.30); MALDI-TOF MS *m/z* calcd for $C_{68}H_8O_3$ $[M]^-$ 872.0479, found 872.0470.

4. NMR Spectra of Compounds 2a–i and 3a–5a

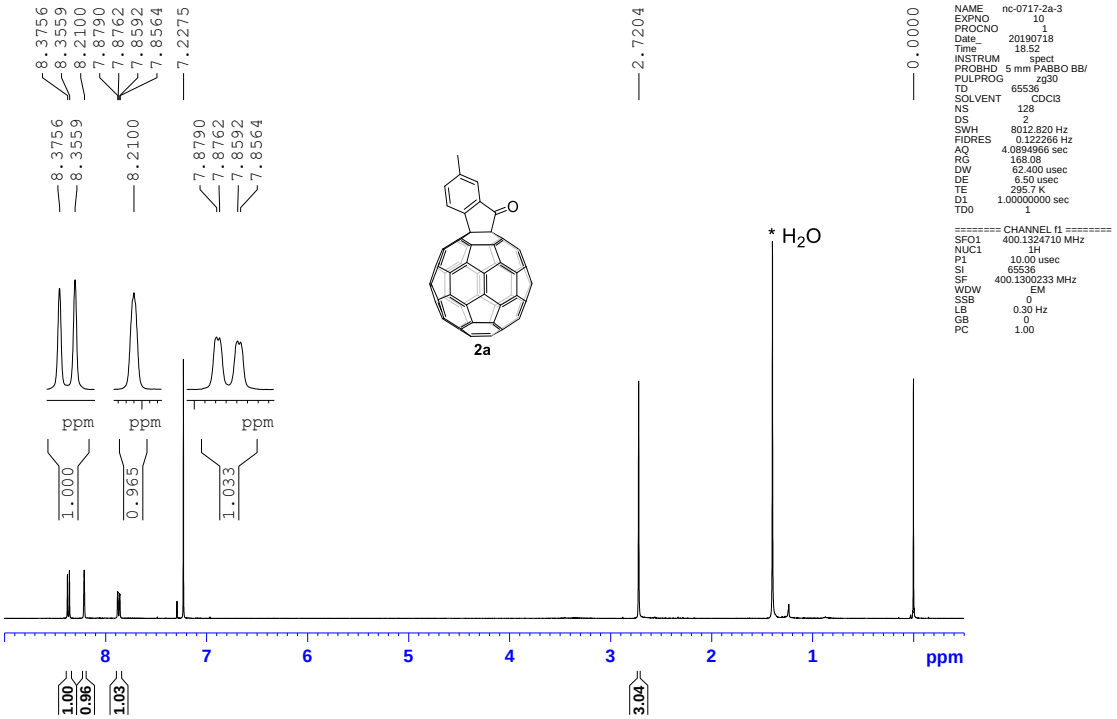

Figure S1. ^{1}H NMR (400 MHz, 1:1 CS_2/$CDCl_3$) of compound **2a**.

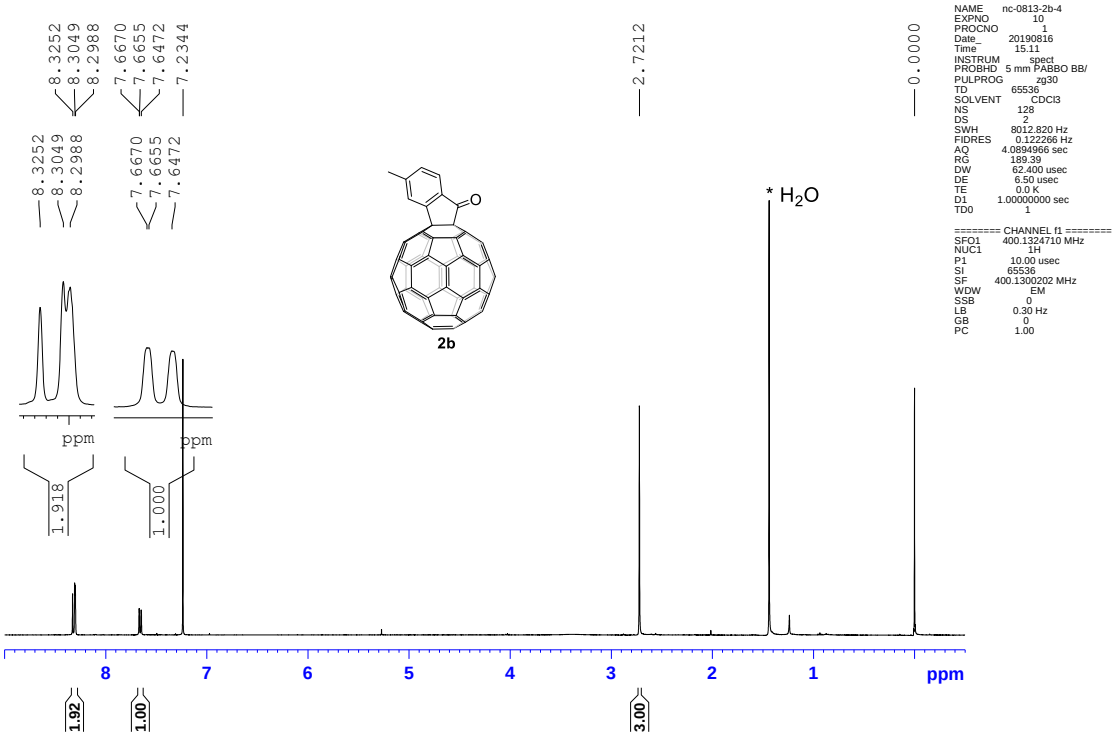

Figure S2. ^{1}H NMR (400 MHz, 1:1 CS_2/$CDCl_3$) of compound **2b**.

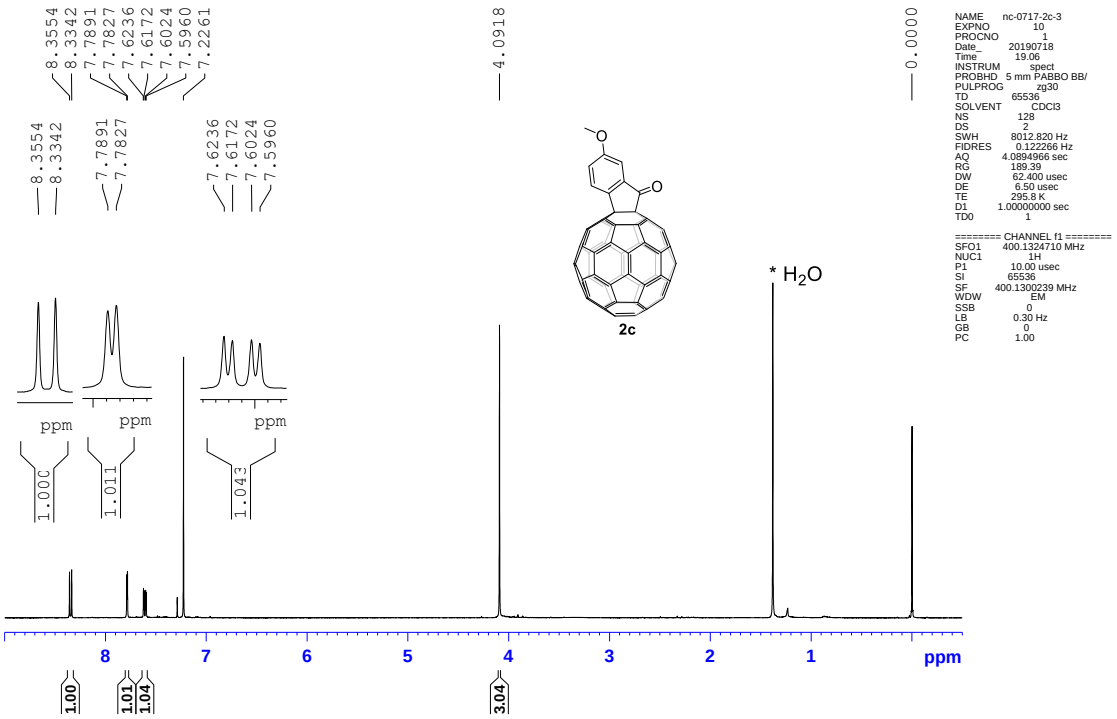

Figure S3. ^{1}H NMR (400 MHz, 1:1 CS_2/$CDCl_3$) of compound **2c**.

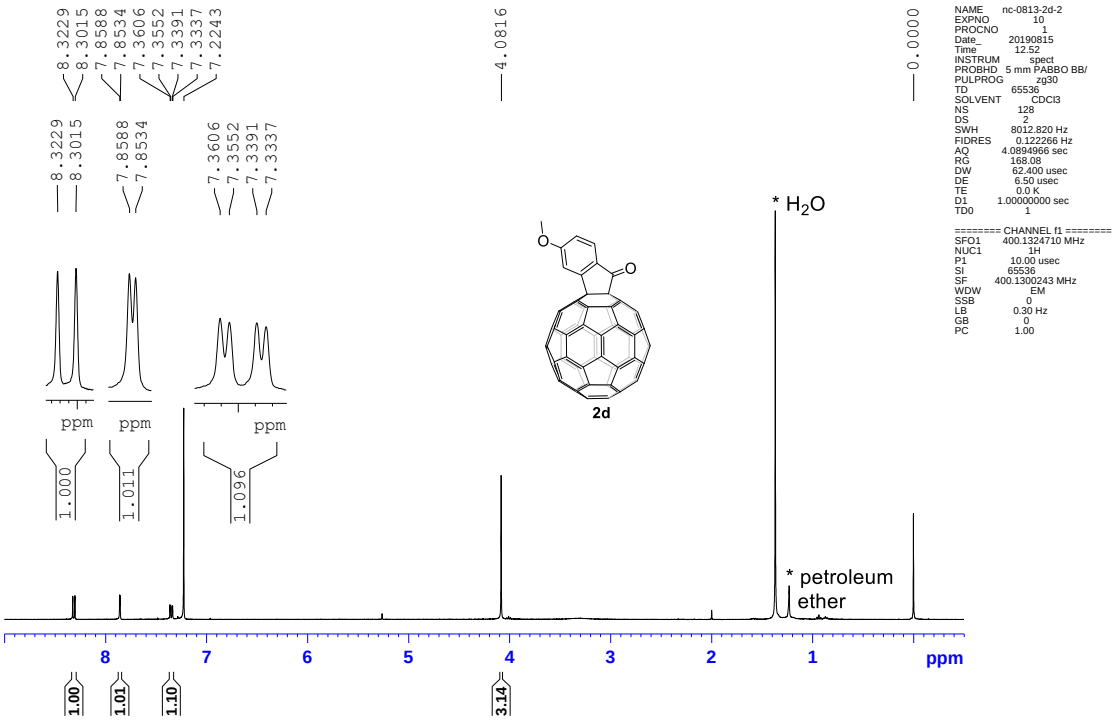

Figure S4. ^{1}H NMR (400 MHz, 1:1 CS_2/$CDCl_3$) of compound **2d**.

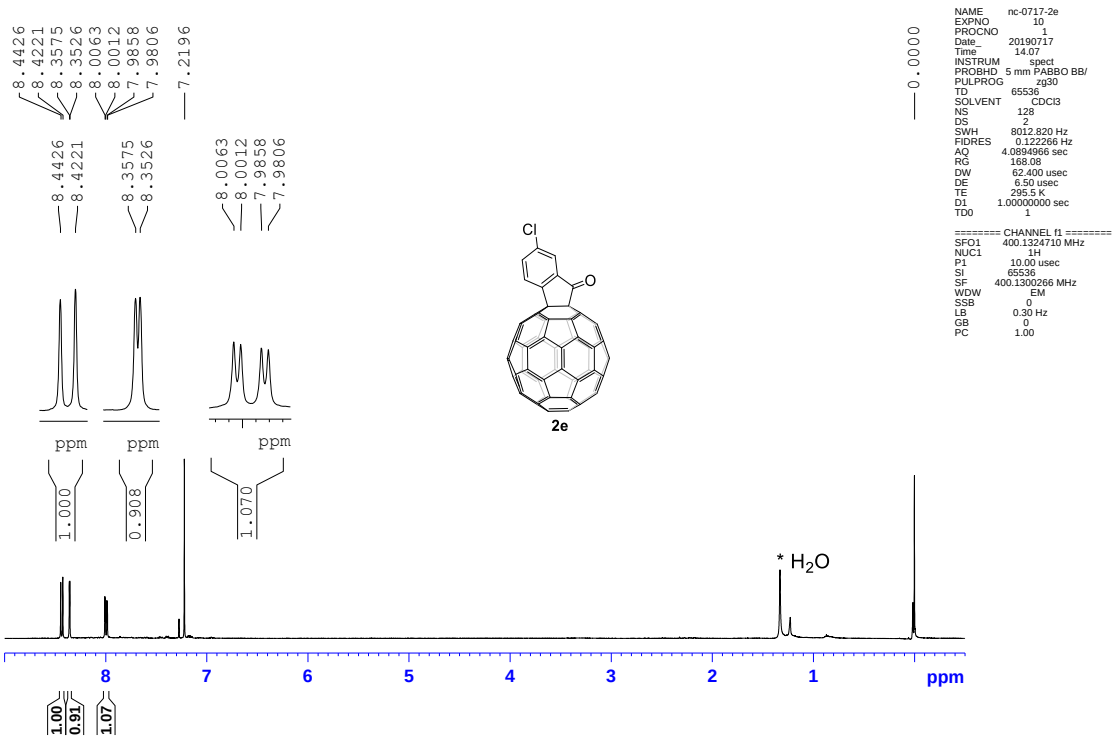

Figure S5. ^{1}H NMR (400 MHz, 1:1 CS_2/$CDCl_3$) of compound **2e**.

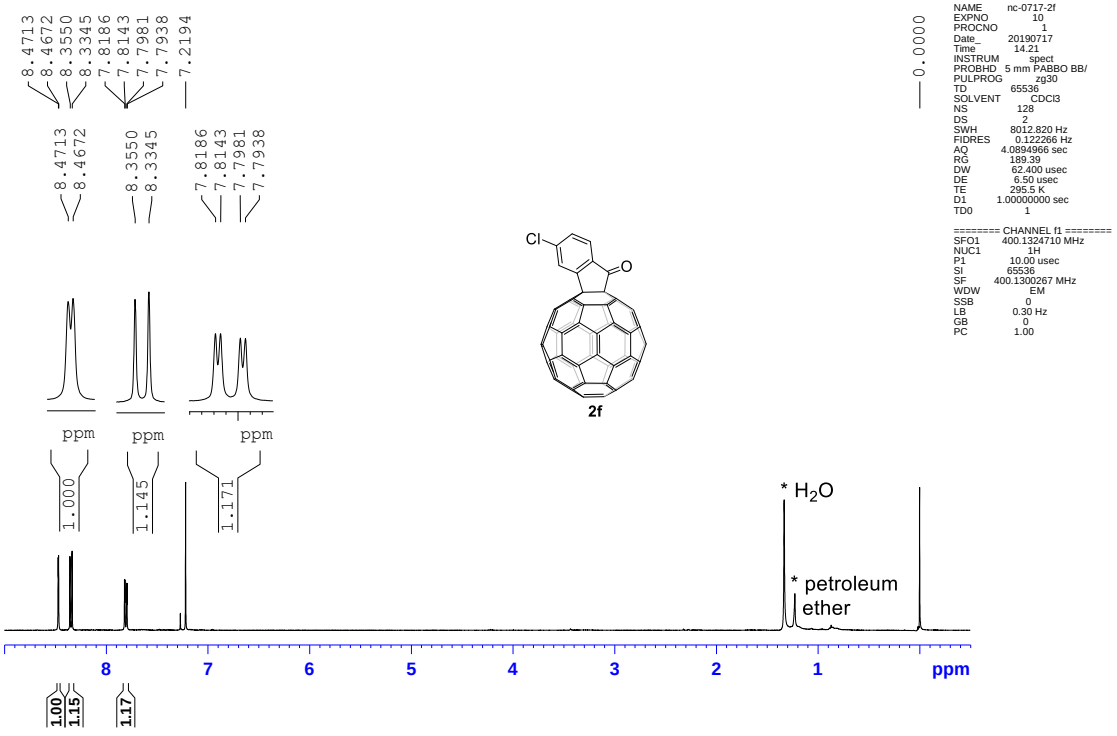

Figure S6. ^{1}H NMR (400 MHz, 1:1 CS_2/$CDCl_3$) of compound **2f**.

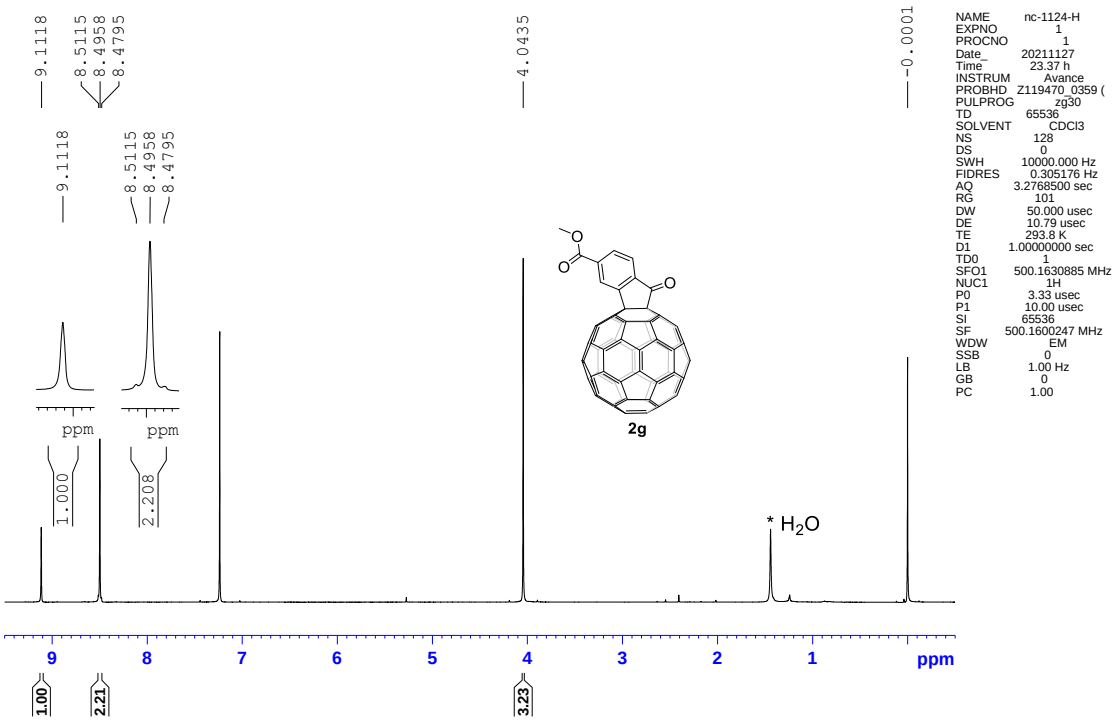

Figure S7. ^{1}H NMR (500 MHz, 1:1 CS_2/$CDCl_3$) of compound **2g**.

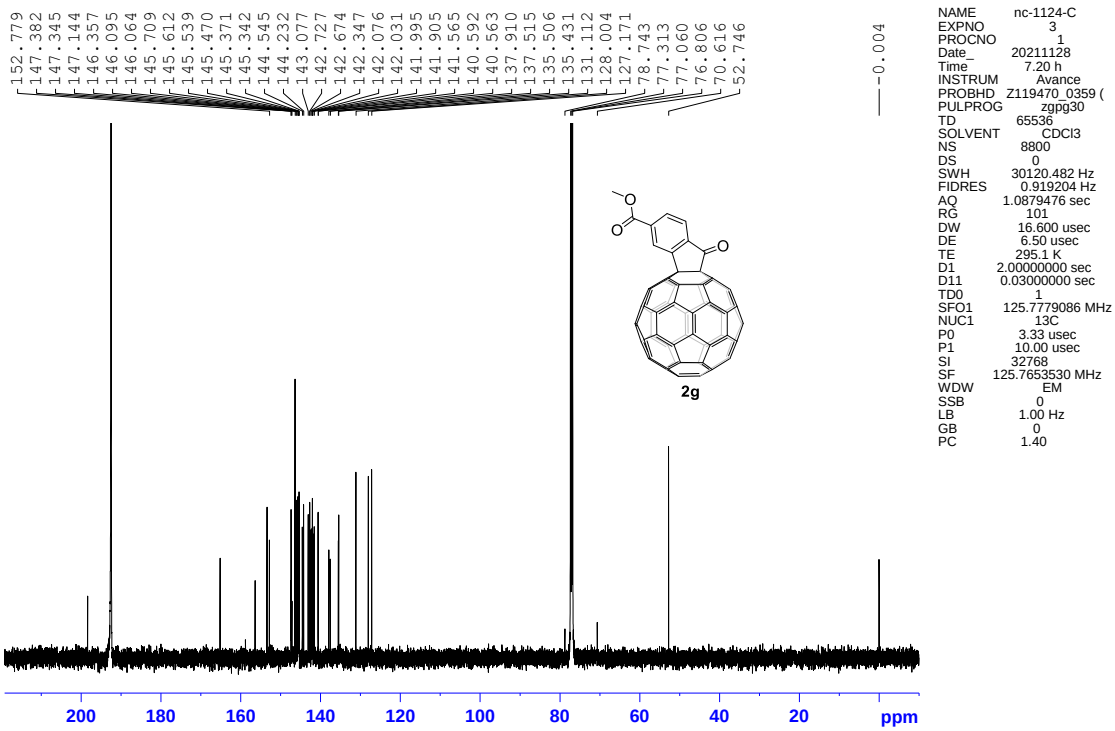

Figure S8. ^{13}C NMR (126 MHz, 1:1 CS_2/$CDCl_3$) of compound **2g**.

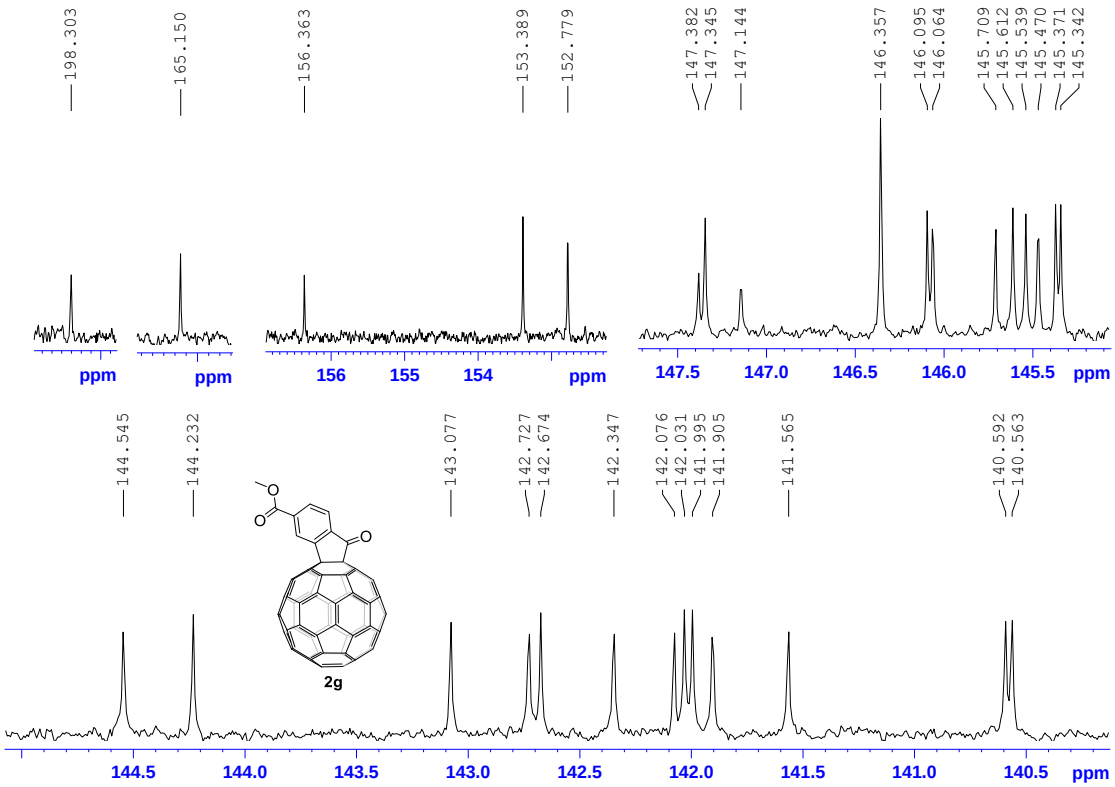

Figure S9. Expanded ^{13}C NMR (126 MHz, 1:1 $CS_2/CDCl_3$) of compound **2g**.

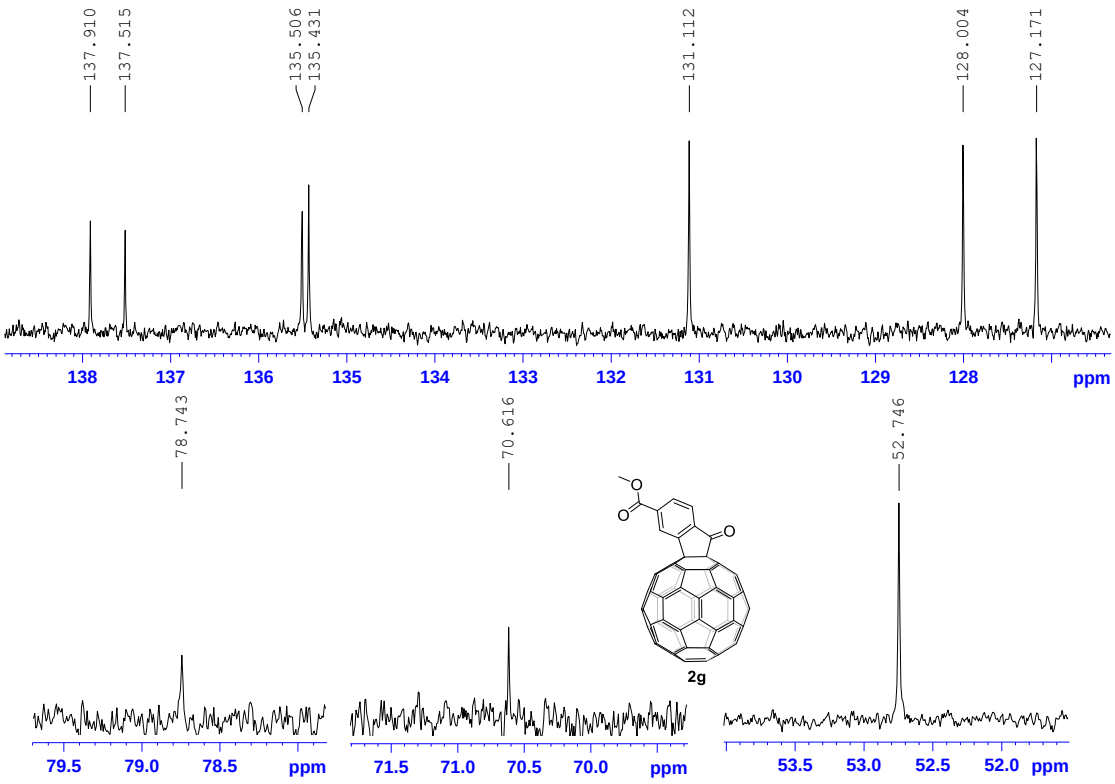

Figure S10. Expanded ^{13}C NMR (126 MHz, 1:1 $CS_2/CDCl_3$) of compound **2g**.

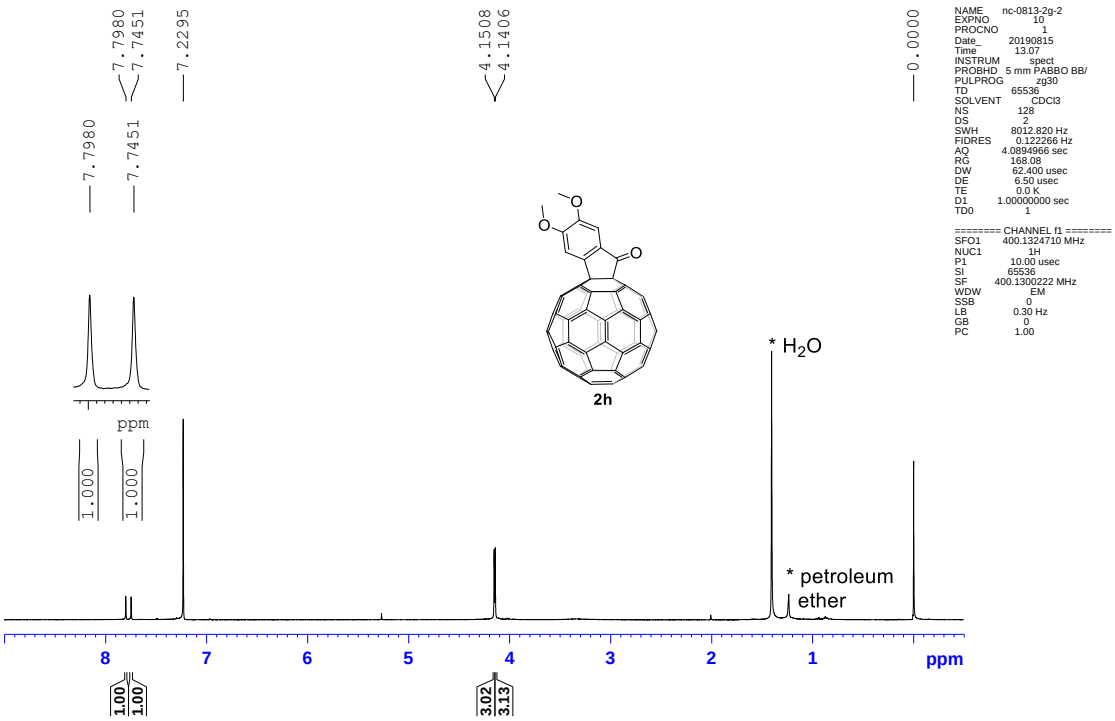

Figure S11. ^{1}H NMR (400 MHz, 1:1 CS_2/$CDCl_3$) of compound **2h**.

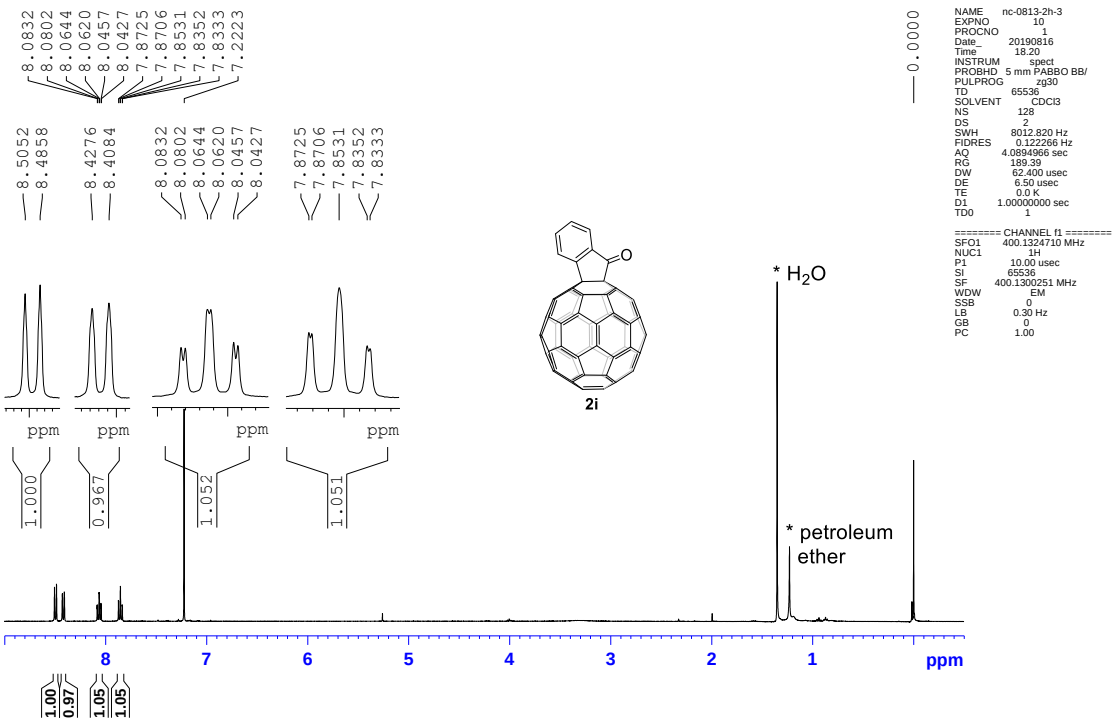

Figure S12. ^{1}H NMR (400 MHz, 1:1 CS_2/$CDCl_3$) of compound **2i**.

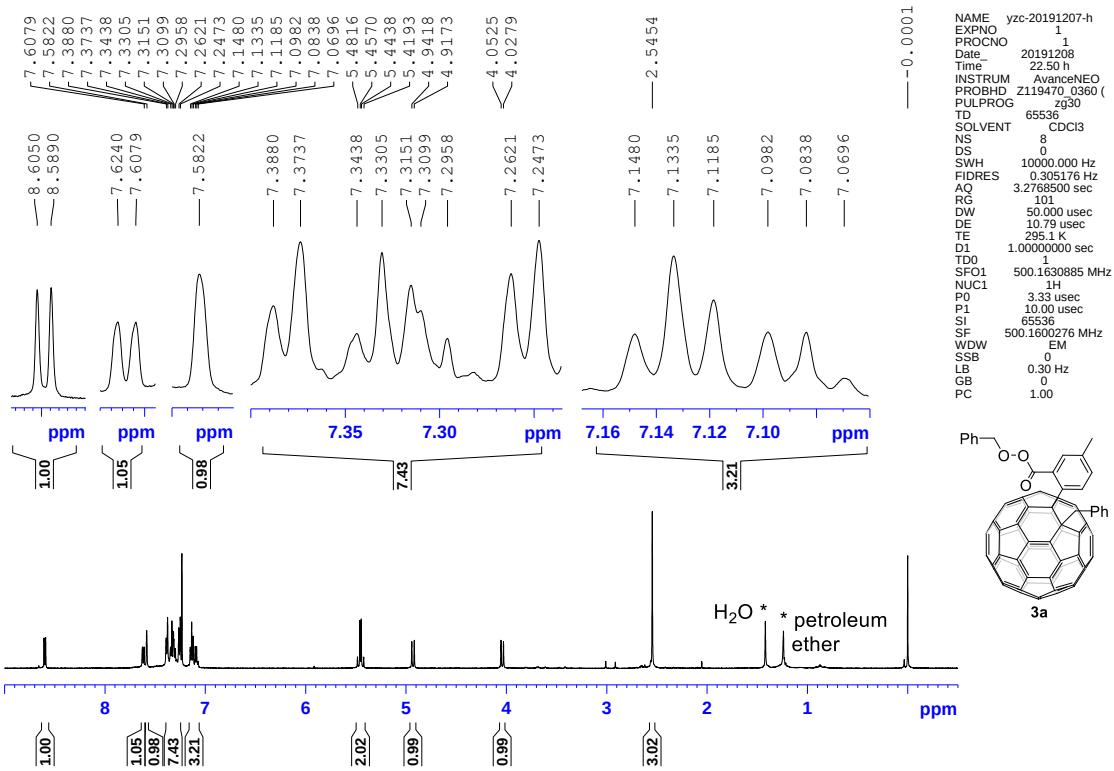

Figure S13. ^{1}H NMR (500 MHz, 1:1 CS_2/$CDCl_3$) of compound **3a**.

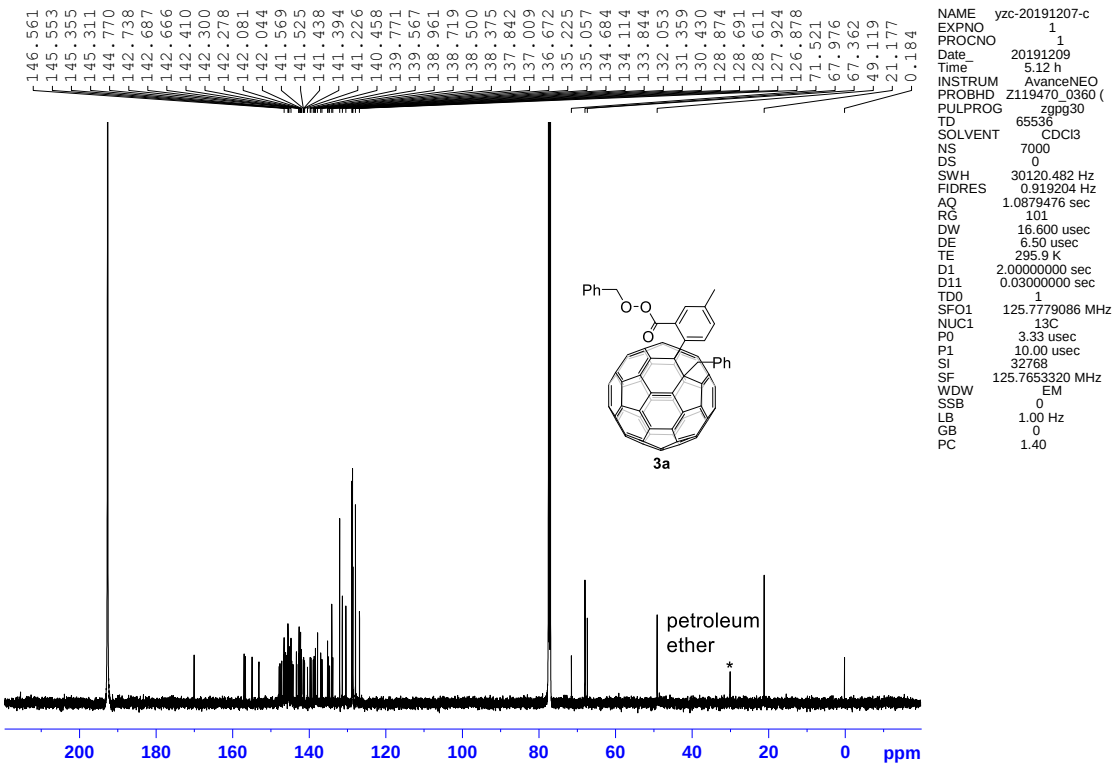

Figure S14. ^{13}C NMR (126 MHz, 1:1 CS_2/$CDCl_3$) of compound **3a**.

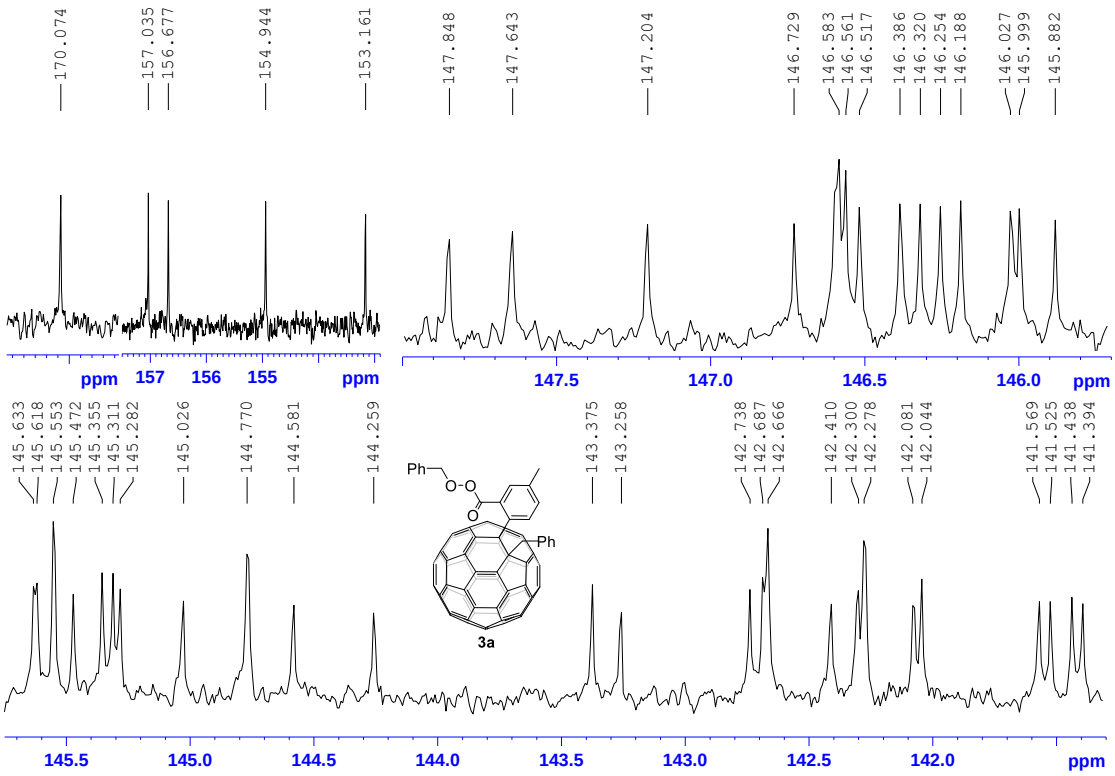

Figure S15. Expanded ^{13}C NMR (126 MHz, 1:1 $CS_2/CDCl_3$) of compound **3a**.

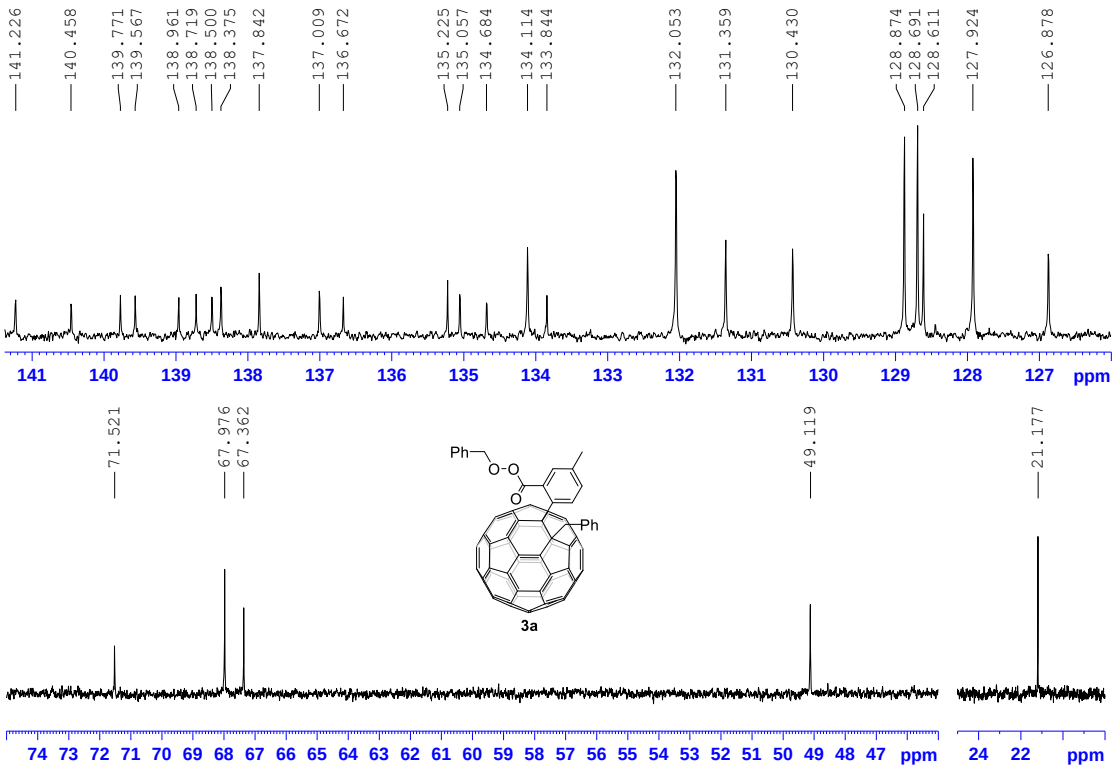

Figure S16. Expanded ^{13}C NMR (126 MHz, 1:1 $CS_2/CDCl_3$) of compound **3a**.

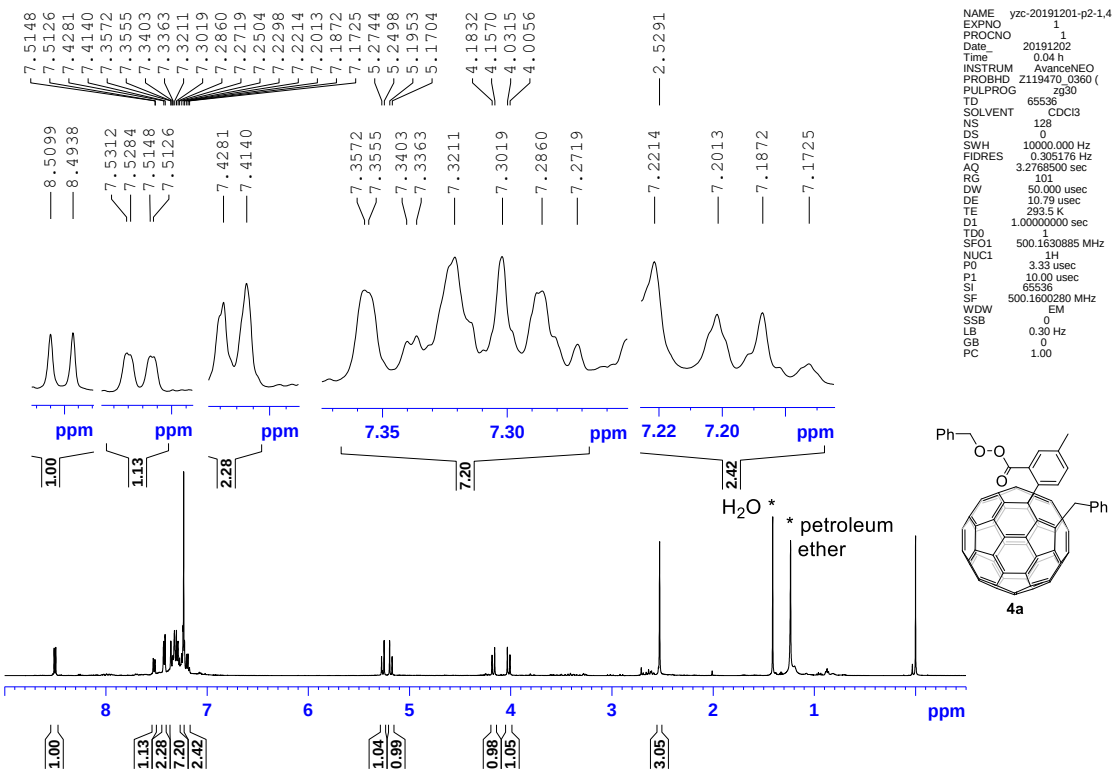

Figure S17. ^{1}H NMR (500 MHz, 1:1 CS_2/$CDCl_3$) of compound **4a**.

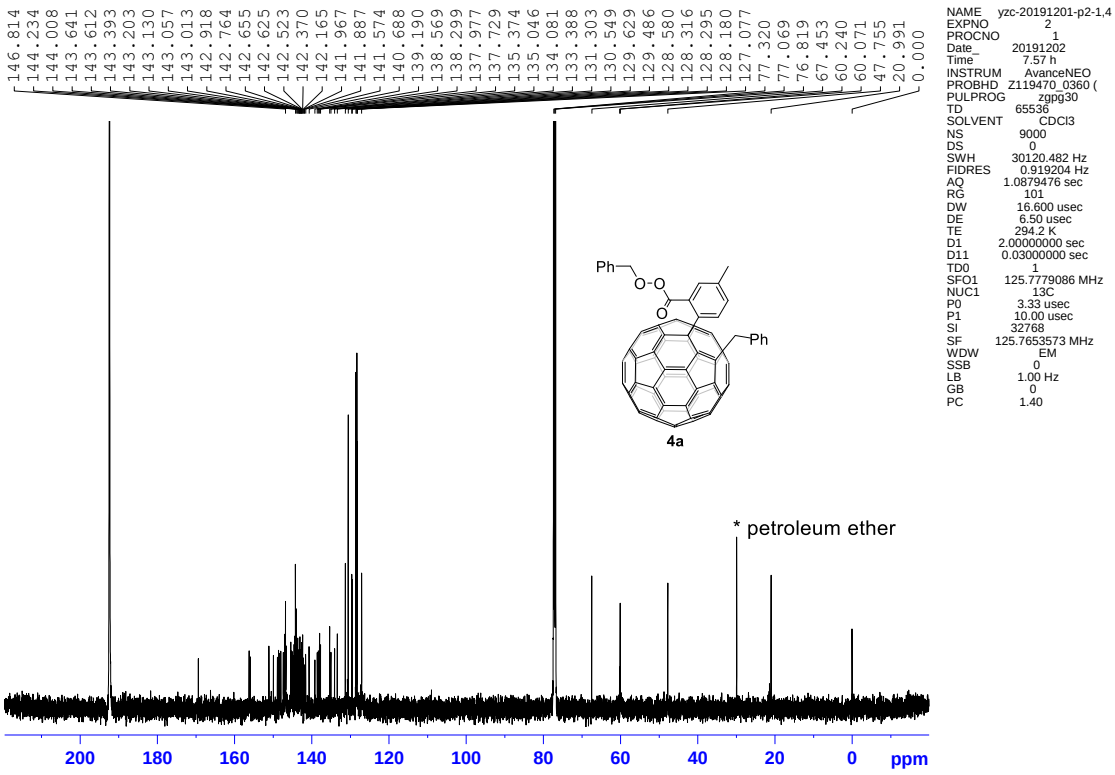

Figure S18. ^{13}C NMR (126 MHz, 1:1 CS_2/$CDCl_3$) of compound **4a**.

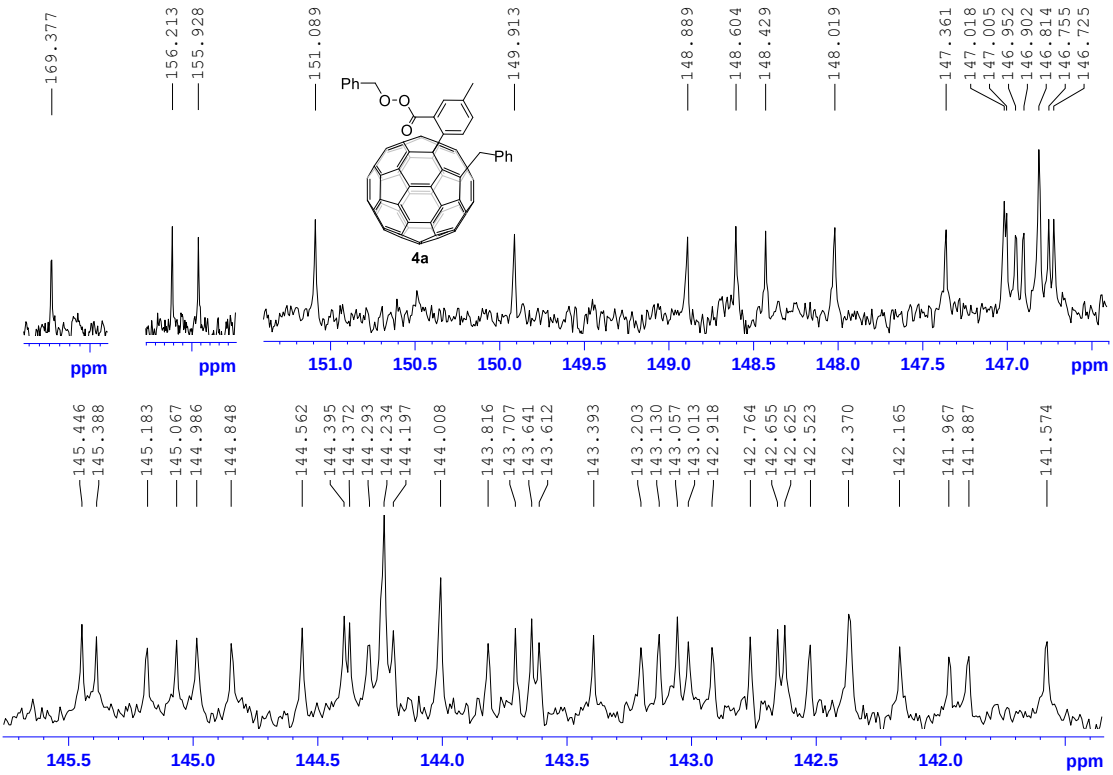

Figure S19. Expanded ^{13}C NMR (126 MHz, 1:1 $CS_2/CDCl_3$) of compound **4a**.

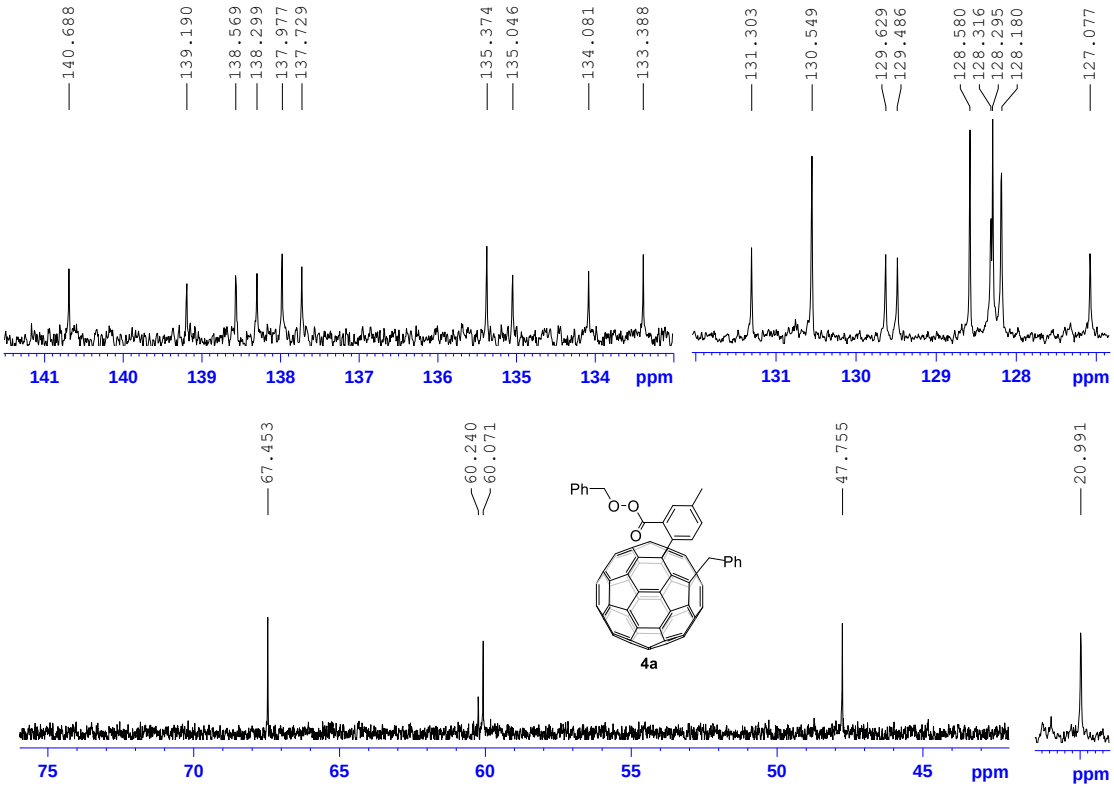

Figure S20. Expanded ^{13}C NMR (126 MHz, 1:1 $CS_2/CDCl_3$) of compound **4a**.

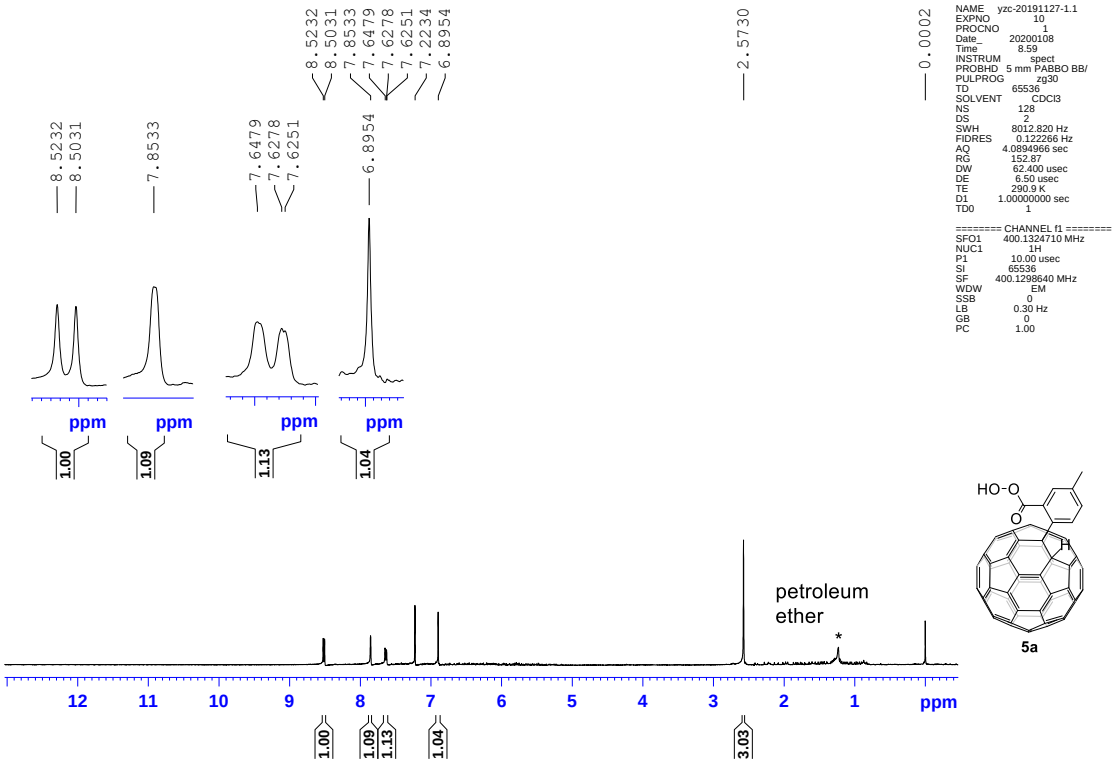

Figure S21. ^{1}H NMR (400 MHz, 1:1 CS_2/$CDCl_3$) of compound **5a**.

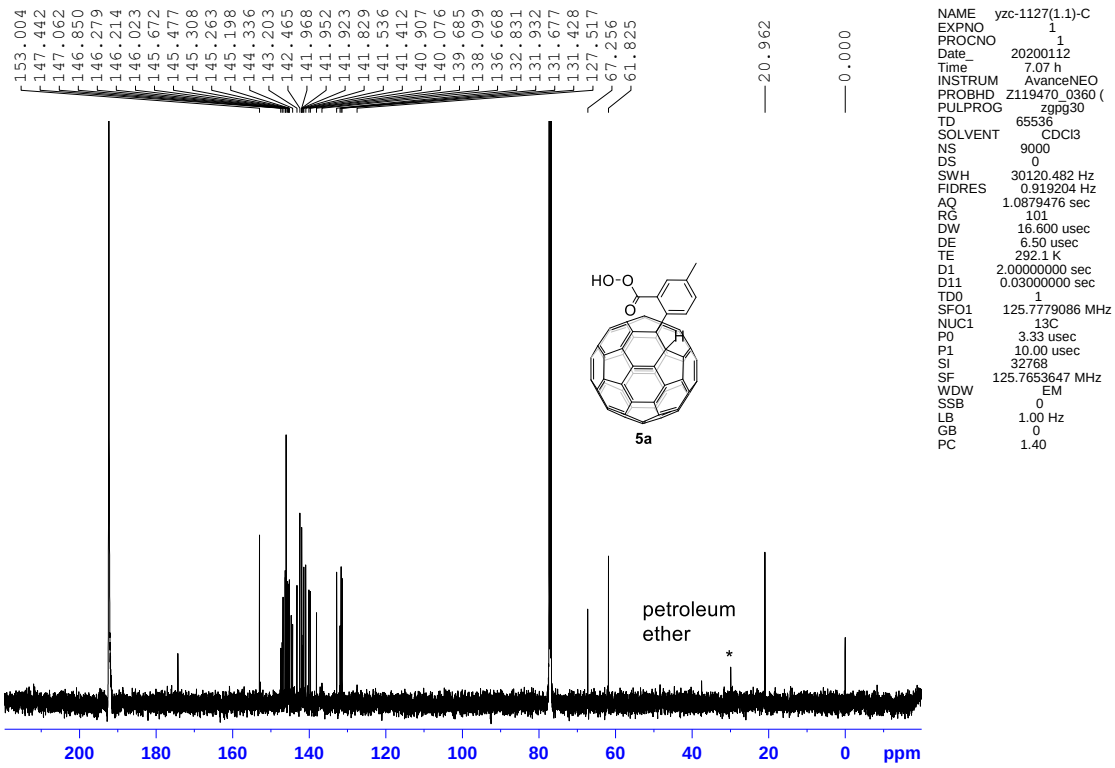

Figure S22. ^{13}C NMR (126 MHz, 1:1 CS_2/$CDCl_3$) of compound **5a**.

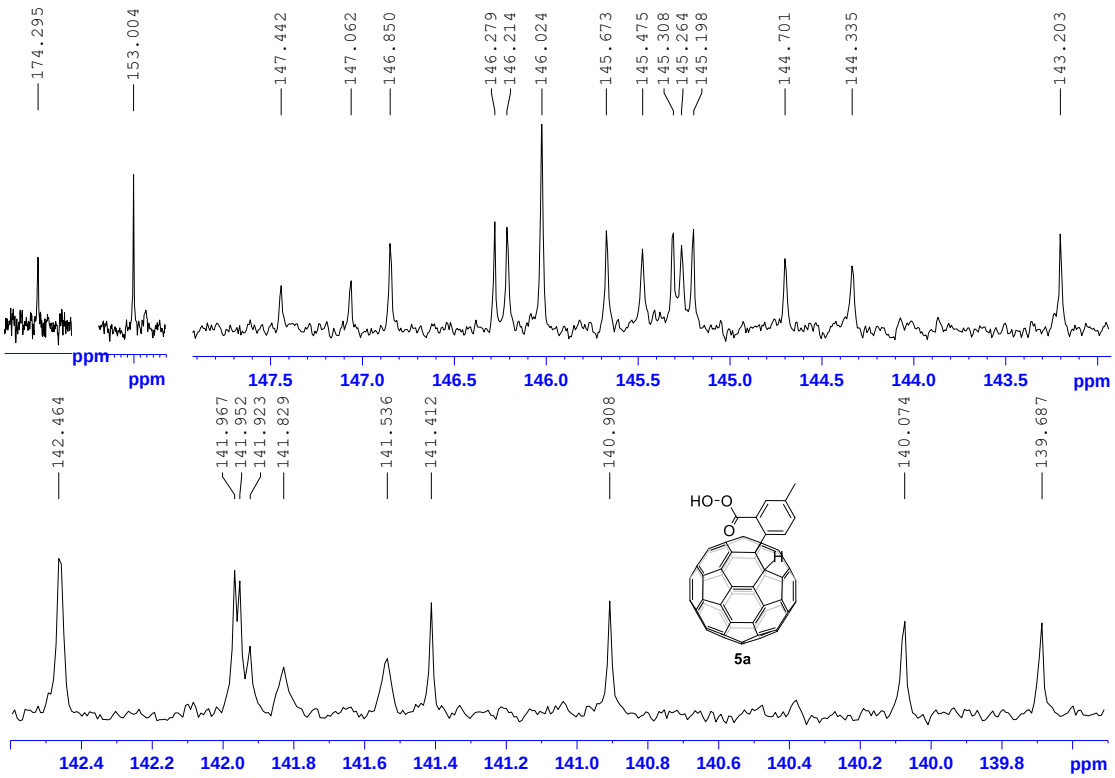

Figure S23. Expanded ^{13}C NMR (126 MHz, 1:1 $CS_2/CDCl_3$) of compound **5a**.

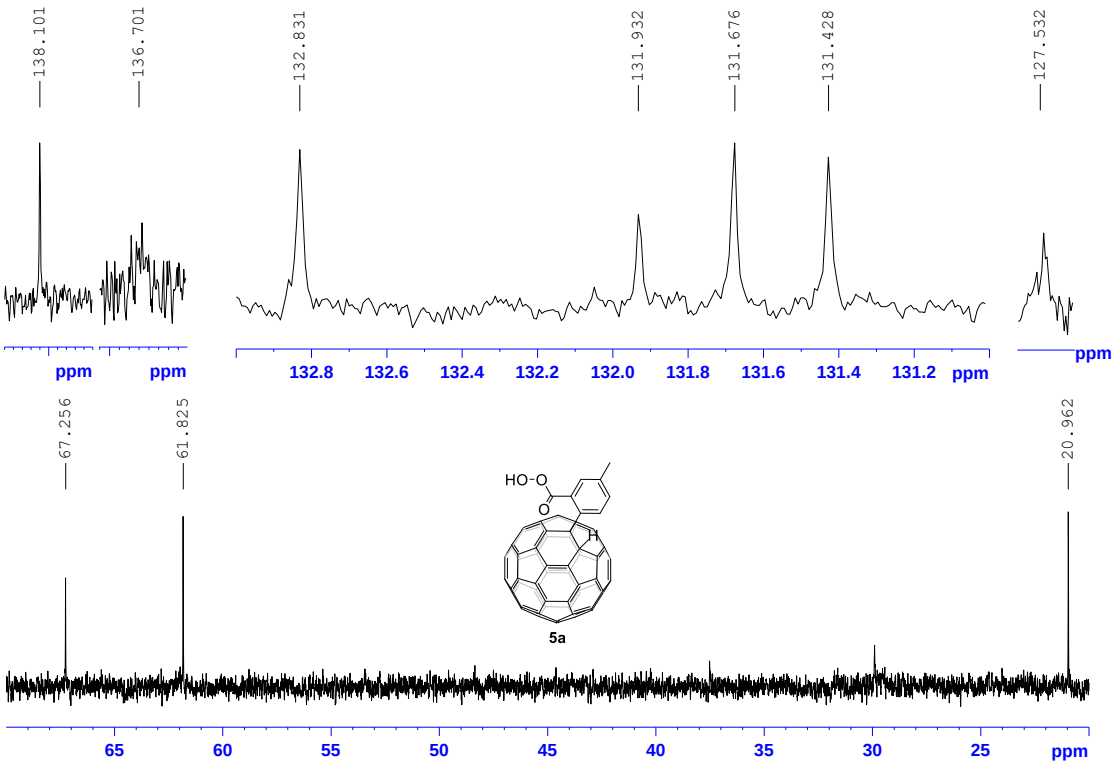

Figure S24. Expanded ^{13}C NMR (126 MHz, 1:1 $CS_2/CDCl_3$) of compound **5a**.

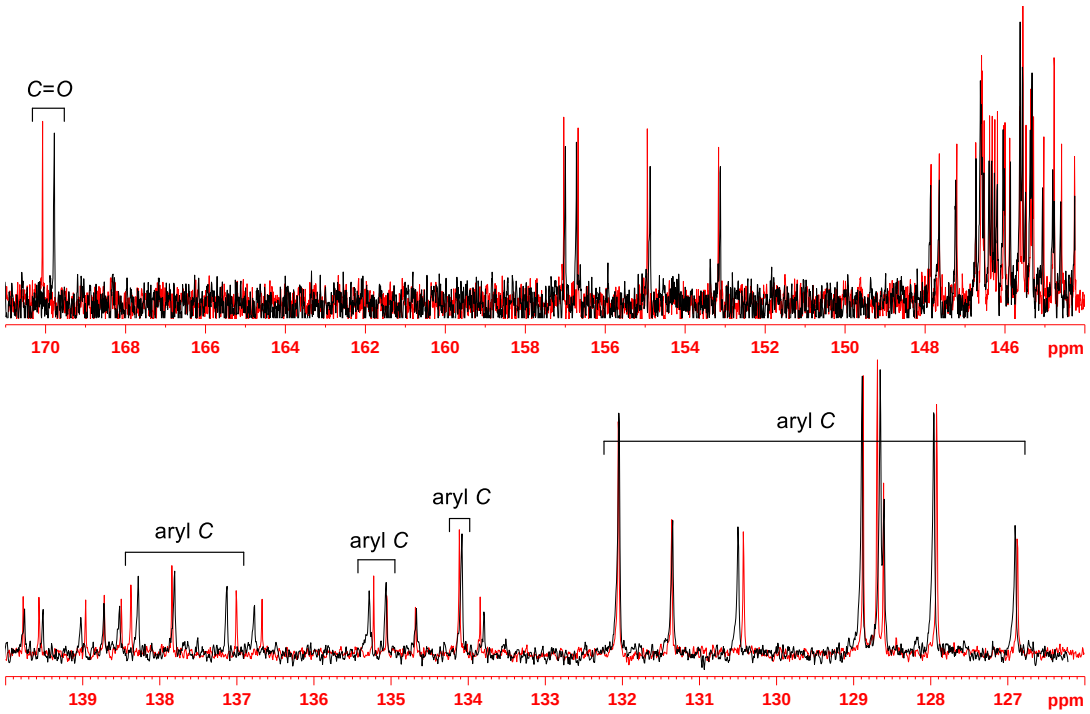

Figure S25. Expanded ^{13}C NMR (126 MHz, 1:1 CS_2/$CDCl_3$) of **3a** (red) and **6**[3] (black) in the regions of 171–144 and 140–126 ppm.

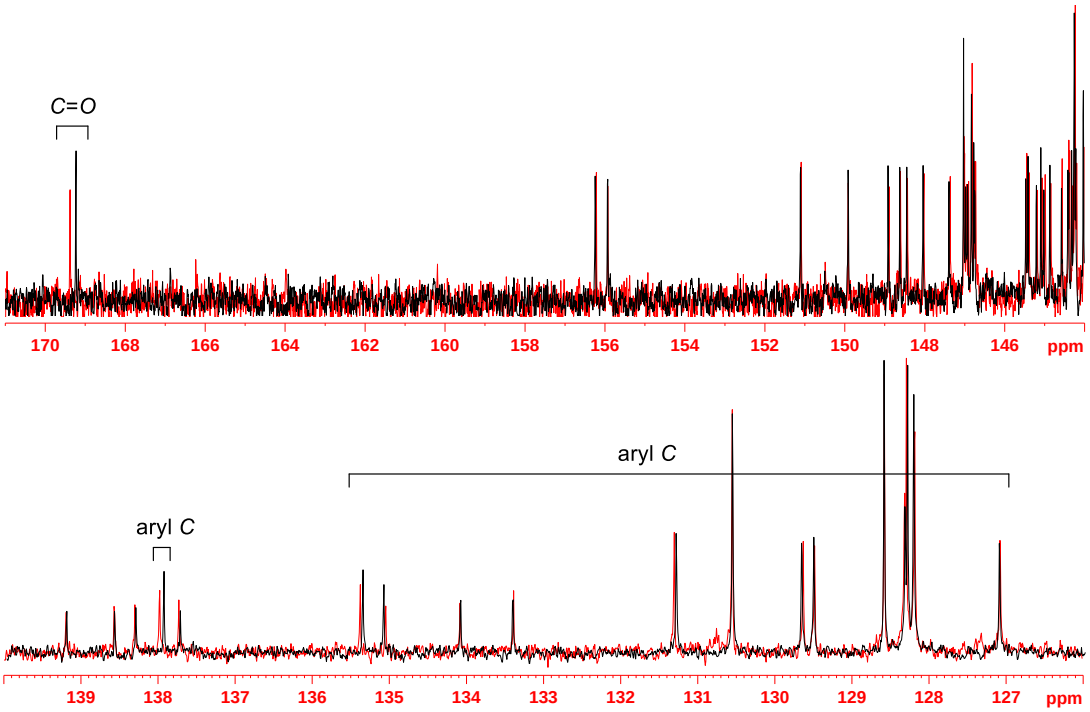

Figure S26. Expanded ^{13}C NMR (126 MHz, 1:1 CS_2/$CDCl_3$) of **4a** (red) and **7**[3] (black) in the regions of 171–144 and 140–126 ppm.

5. UV-vis Spectra of Compounds 2g and 3a–5a

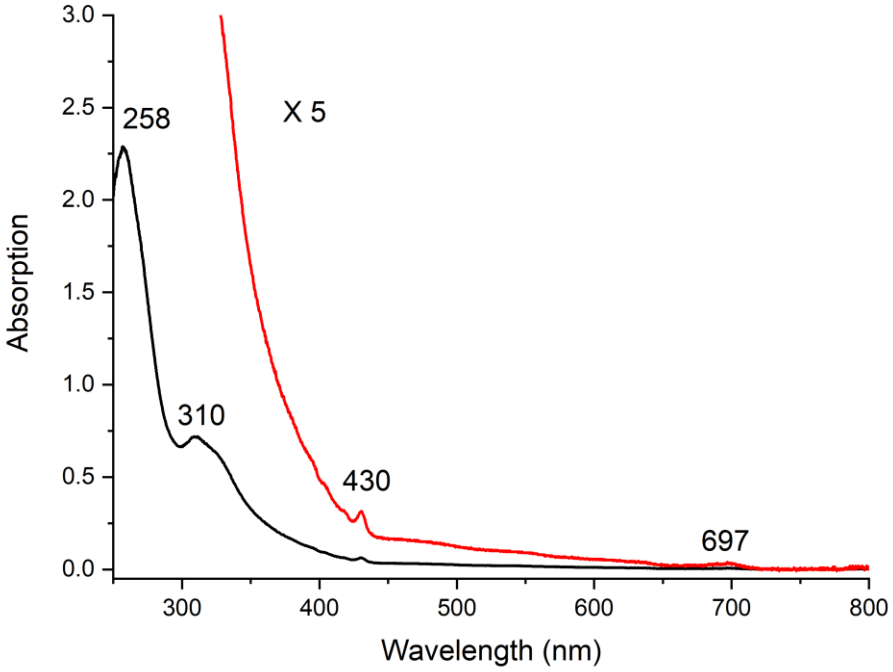

Figure S27. UV-vis absorption of **2g** in $CHCl_3$.

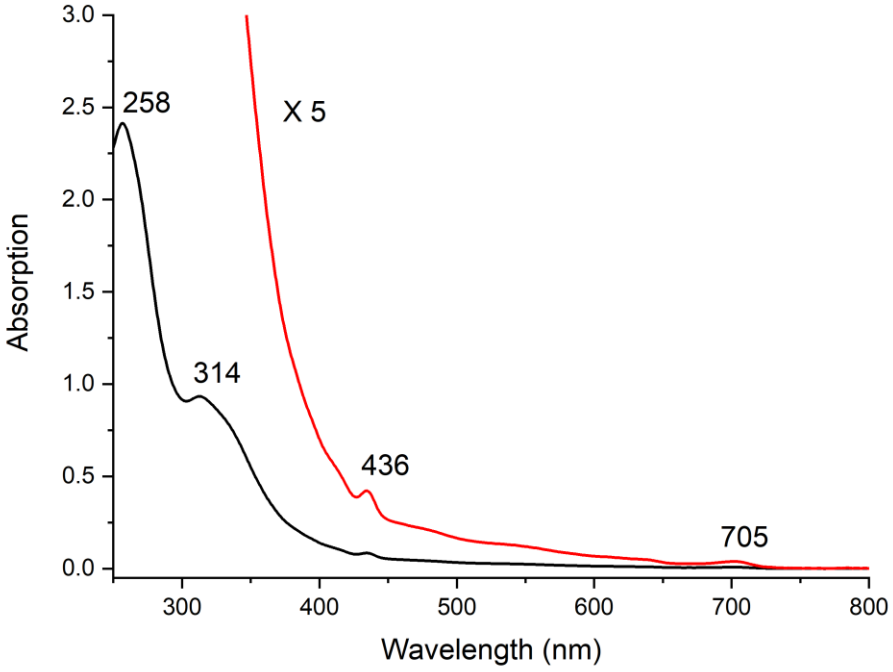

Figure S28. UV-vis absorption of **3a** in $CHCl_3$.

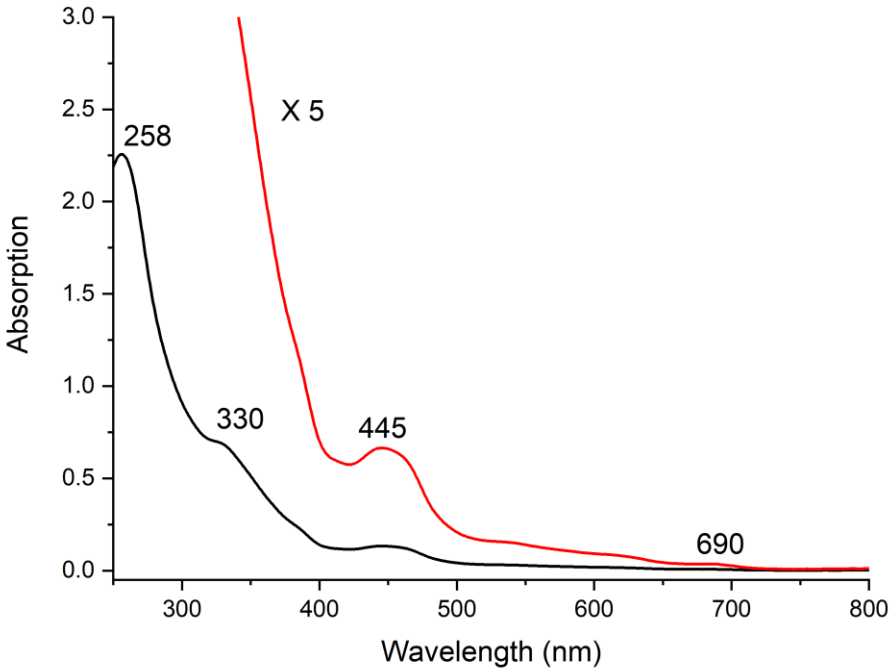

Figure S29. UV-vis absorption of **4a** in $CHCl_3$.

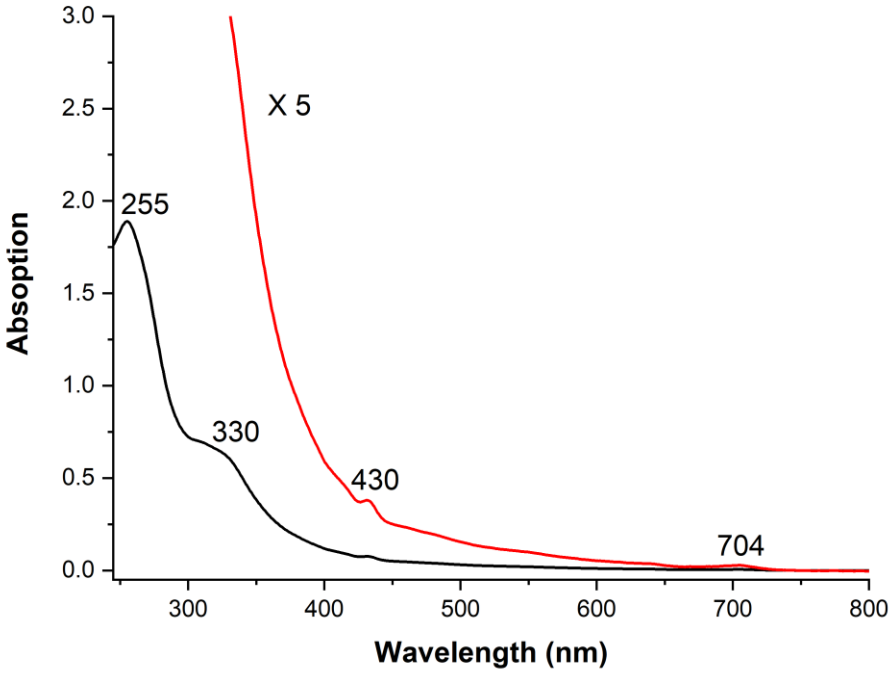

Figure S30. UV-vis absorption of **5a** in $CHCl_3$.

6. MALDI-TOF HRMS Spectra of Compounds 2g and 3a–5a

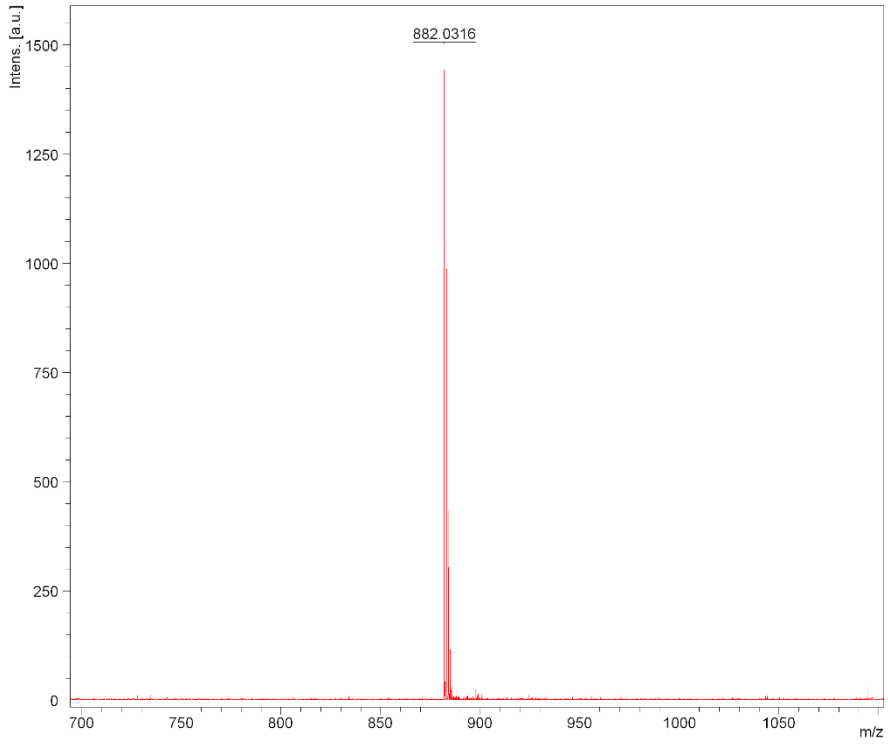

Figure S31. MALDI-TOF HRMS of **2g**.

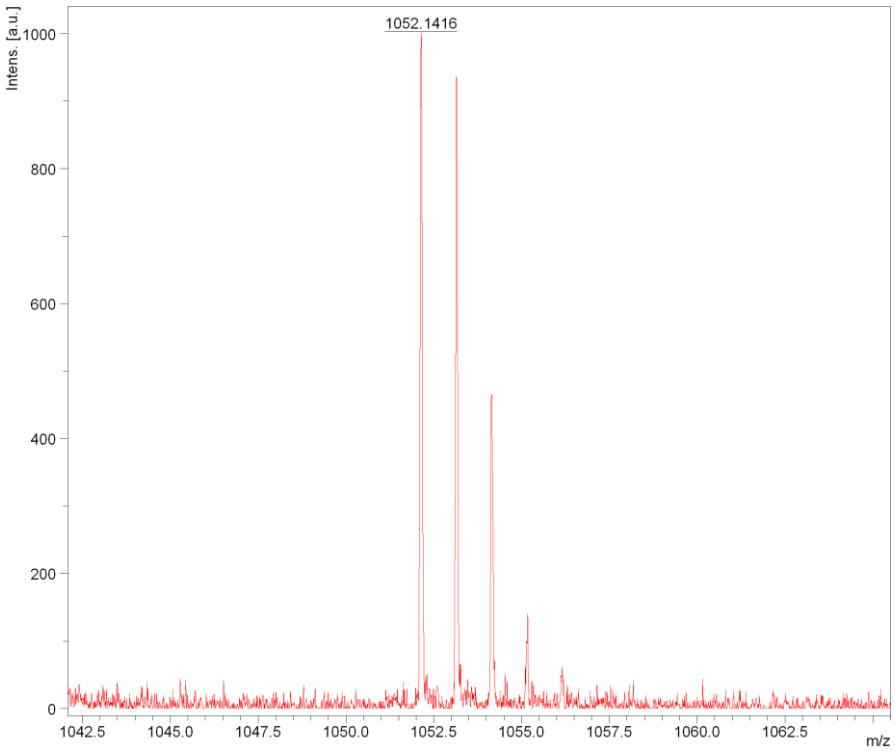

Figure S32. MALDI-TOF HRMS of **3a**.

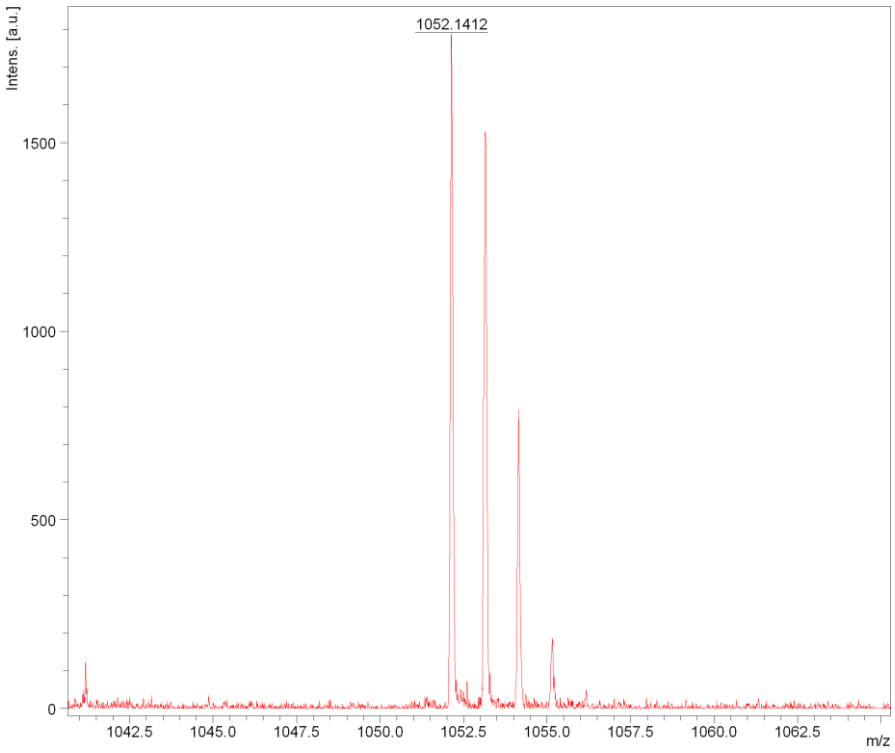

Figure S33. MALDI-TOF HRMS of **4a**.

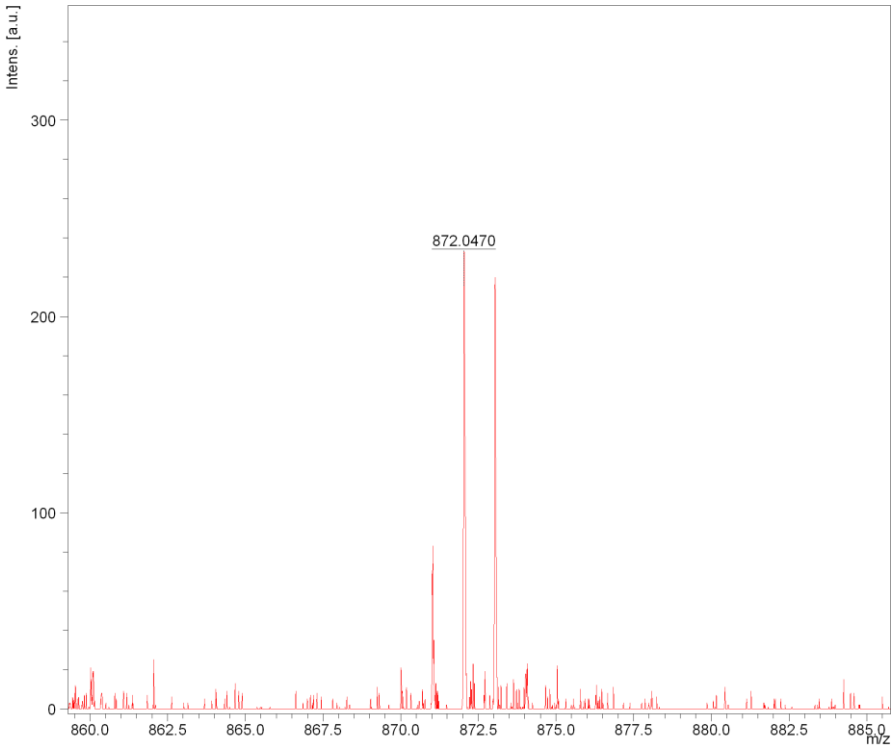

Figure S34. MALDI-TOF HRMS of **5a**.

7. CVs and DPVs of 2g and 3a–5a

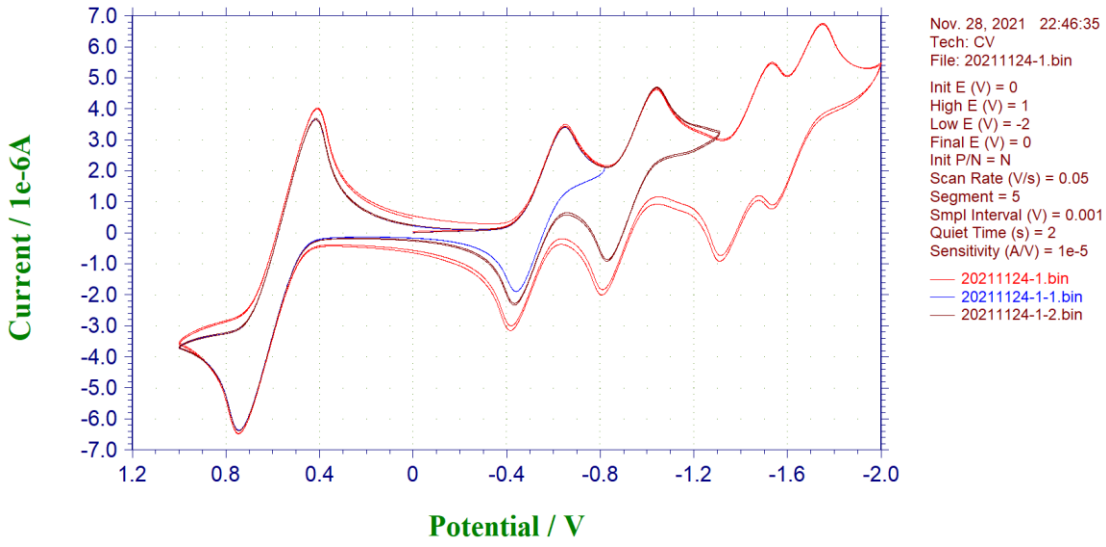

Figure S35. Cyclic voltammogram of **2g** (scanning rate: 50 mV s^{-1}).

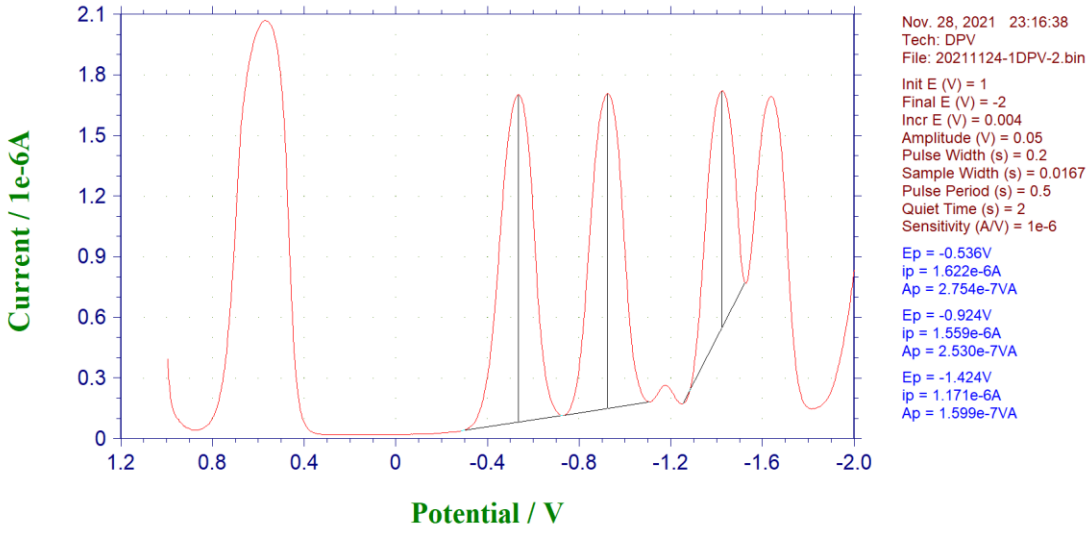

Figure S36. Differential pulse voltammogram of **2g**.

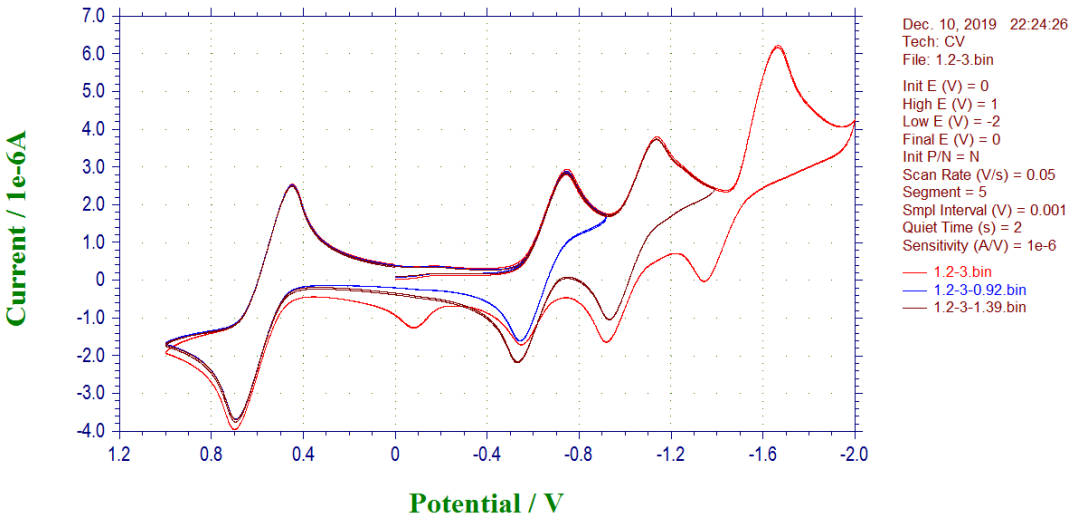

Figure S37. Cyclic voltammogram of **3a** (scanning rate: 50 mV s^{-1}).

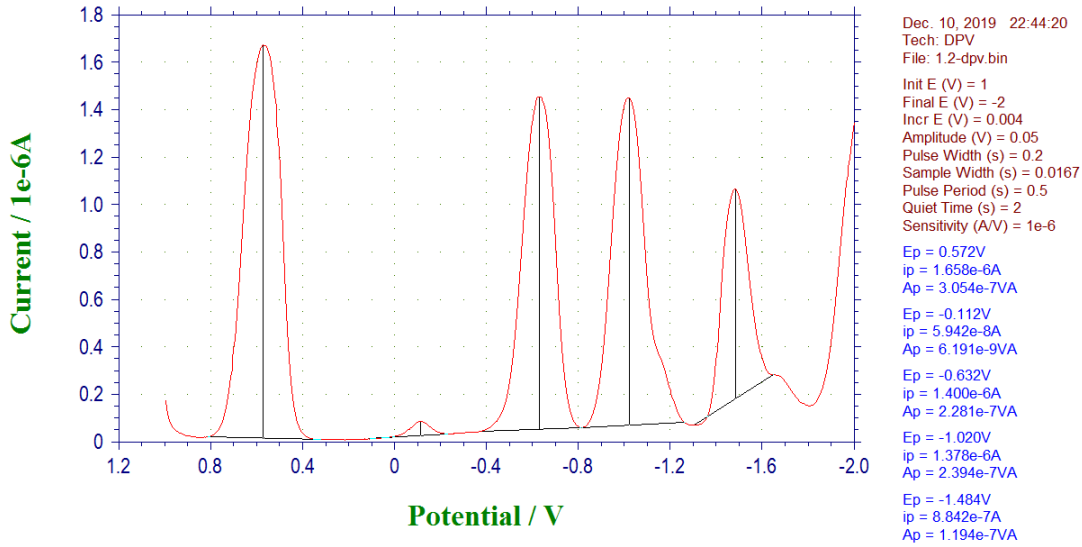

Figure S38. Differential pulse voltammogram of **3a**.

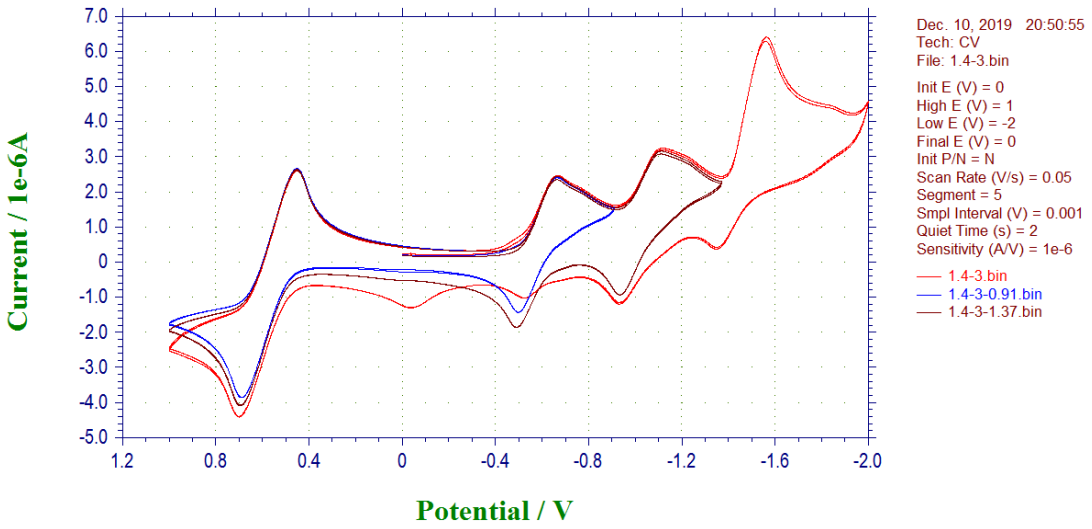

Figure S39. Cyclic voltammogram of **4a** (scanning rate: 50 mV s^{-1}).

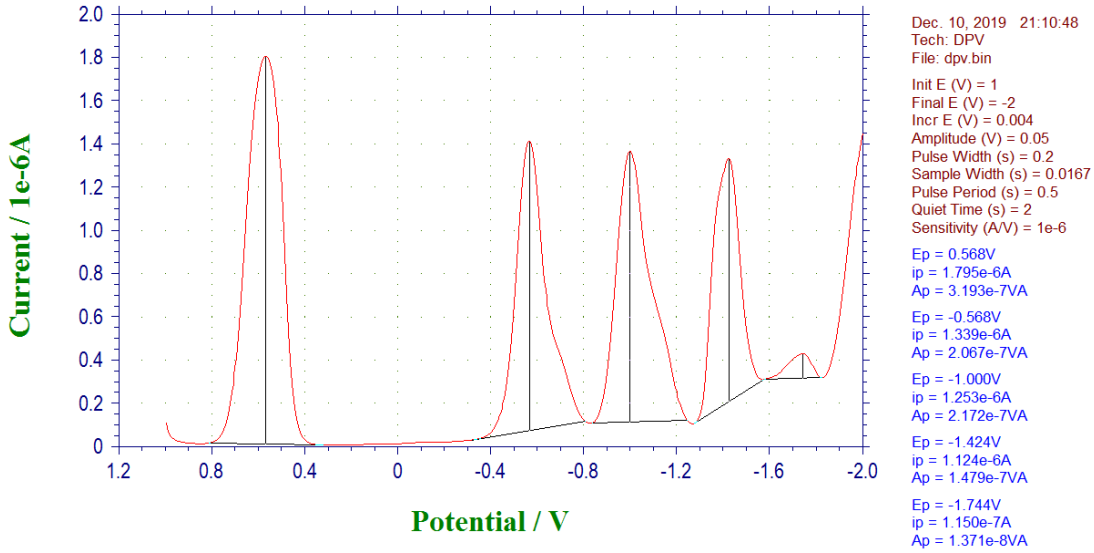

Figure S40. Differential pulse voltammogram of **4a**.

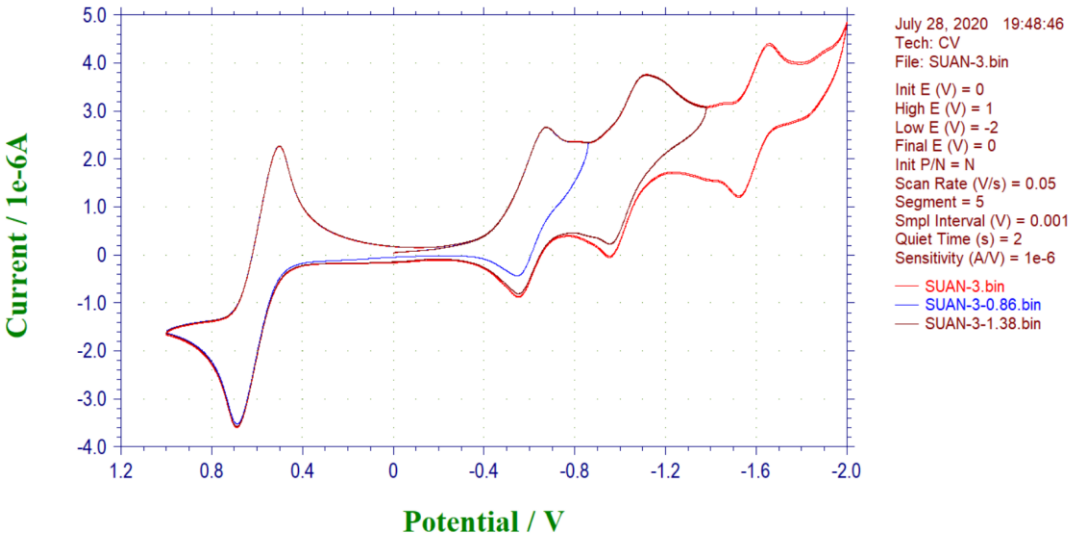

Figure S41. Cyclic voltammogram of **5a** (scanning rate: 50 mV s^{-1}).

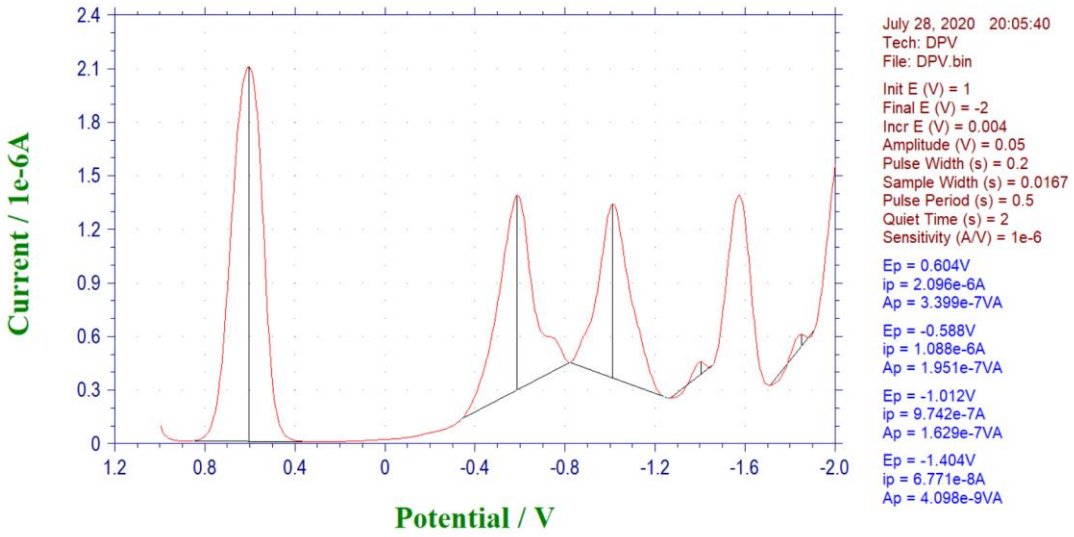

Figure S42. Differential pulse voltammogram of **5a**.

8. References

1 G.-W. Wang and B. Zhu, *Chem. Commun.*, 2009, 1769–1771.

2 C. Niu, D.-B. Zhou, Y. Yang, Z.-C. Yin and G.-W. Wang, *Chem. Sci.*, 2019, **10**, 3012–3017.

3 C. Niu, B. Li, Z.-C. Yin, S. Yang and G.-W. Wang, *Org. Lett.*, 2019, **21**, 7346–7350.